BioRadiations

A Resource for Life Science Research Number 116

Cover Story

RNAi: Delivery to Detection

Features

What's New

BIO-RAD

A Field of Choice

Paint a vivid picture with the Bio-Plex™ system — offering a broad selection of multiplex cytokine assays.*

The power of xMAP multiplexing allows you to test a full range of cytokines with as little as 12 µl of sample — saving precious samples and time.

- **Various applications:** human, mouse, and rat samples
- **Choice of matrices:** serum, plasma, and cell culture supernatants
- **Ready-to-use** assays, reagents, and diluents
- **Mixed-to-order** assay services

For more information, visit **www.bio-rad.com/bio-plex/**

1. Cytokine panel or singleplex assay

2. Cytokine reagent kit

3. Optional diluent kit

NEW TARGETS AVAILABLE

Assays	Human	Mouse	Rat
IL-1α		●	●
IL-1β	●	●	●
IL-2	●	●	●
IL-3		●	
IL-4	●	●	●
IL-5	●	●	
IL-6	●	●	●
IL-7	●		
IL-8	●		
IL-9		●	
IL-10	●	●	●
IL-12 (p40)		●	
IL-12 (p70)	●	●	
IL-13	●	●	
IL-17	●	●	
Eotaxin		●	
G-CSF	●	●	
GM-CSF	●	●	●
IFN-γ	●	●	●
KC		●	
MCP-1 (MCAF)	●	●	
MIP-1α		●	
MIP-1β	●	●	
RANTES		●	
TNF-α	●	●	●

* Bio-Plex assays can be run on a Luminex 100 analyzer as well as the Bio-Plex suspension array system.

BioRadiations magazine is published by
Bio-Rad Laboratories, Inc.
2000 Alfred Nobel Drive
Hercules, CA 94547 USA

Bio-Rad Subsidiary
Telephone Numbers

Australia 61-2-9914-2800
Austria 43-1-877-89-01
Belgium 32-9-385-55-11
Brazil 55-21-2527-3454
Canada 00-1-905-712-2771
China 86-21-6305-2255
Czech Republic 420-2-41-43-05-32
Denmark 45-44-52-10-00
Finland 358-9-804-22-00
France 33-1-47-95-69-65
Germany 49-89-318-84-0
Hong Kong 852-2-789-3300
Hungary 36-1-455-8800
India 91-124-239-8112
Israel 972-3-951-4127
Italy 39-2-21609-1
Japan 81-3-5811-6270
Korea 82-2-3473-4460
Latin America 00-1-305-894-5950
Mexico 55-52-00-05-20
The Netherlands 31-318-540666
New Zealand 64-9-415-2280
Norway 47-23-38-41-30
Poland 48-22-331-99-99
Portugal 351-21-472-7700
Russia 7-095-721-1404
Singapore 65-6415-3188
South Africa 27-11-4428508
Spain 34-91-590-5200
Sweden 46-8-555-12700
Switzerland 41-61-717-9555
Taiwan 88-62-2578-7189
Thailand 662-651-8311
United Kingdom 44-20-8328-2000
USA Toll free 1-800-4BIORAD
(1-800-424-6723)

discover.bio-rad.com

On the cover:
Conceptual illustration
of RNAi.
Illustration courtesy of Megan Rojas.

in this issue

BioRadiations 116, 2005

TO OUR READERS

RNA interference (RNAi) is a natural process that has greatly benefited the study of gene function, biological pathways, and drug development, through its use in gene knockdown experiments. Successful application of this powerful tool requires efficient transfer of small interfering RNAs into cells and subsequent verification of the gene knockdown. Our cover story, written by members of our gene expression team, alerts you to the issues to consider when optimizing RNAi experiments. In this article, you will also be introduced to some of the products Bio-Rad has developed to help your experiments run smoothly.

COVER STORY

DEPARTMENTS

TECHNICAL REPORTS

Legal Notices

The 2-D Doctor Is In — 24 Hours a Day, 7 Days a Week

Bio-Rad offers a new worldwide technical support service for expression proteomics applications. Now you can get expert 2-D troubleshooting advice 24 hours a day, 7 days a week online. Our new support tool, the 2-D Doctor, features a collection of problematic 2-D gel images along with their likely causes and suggested remedies. This extensive database is updated as more examples of 2-D gel problems are identified. For easy access if you're not connected to the Web, the 2-D Doctor is also available as a downloadable file and updated regularly.

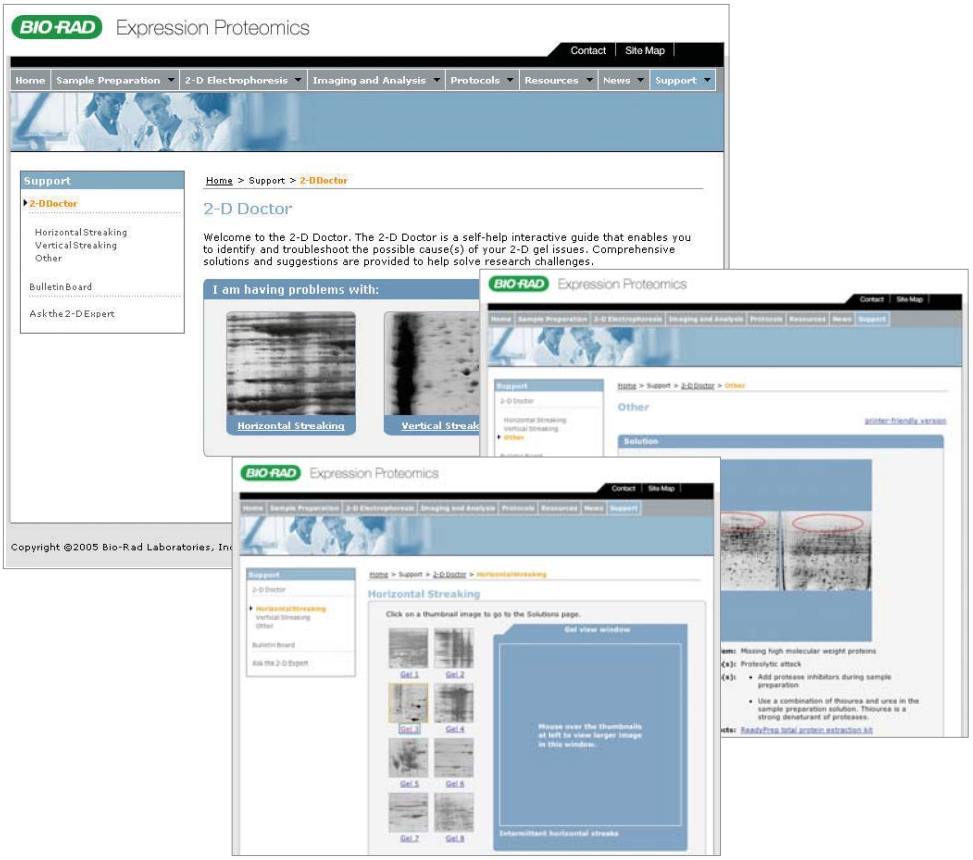

If after viewing the 2-D Doctor you are still not able to resolve your gel problem, you may electronically submit your question to a 2-D expert. Our 2-D expert is committed to responding within 24 hours.*

Another support tool available to you is the ability to correspond with other Bio-Rad customers through our new expression proteomics bulletin board. This is an open forum for you to voice your concerns and raise product issues with other scientists in the proteomics community.

All of these new features can be found at **www.expressionproteomics.com**. Make Bio-Rad your trusted advisor to help solve your expression proteomics research problems.

* 24 hours from receipt of question during normal Pacific time business hours

PowerPac™ HV Power Supply

Drive Your High-Voltage Applications

The PowerPac HV high-voltage power supply supports an increased output of 5,000 V, 500 mA, or 400 W, which allows you to drive all high-voltage applications, including low-current applications in the microampere range. It is ideal for isoelectric focusing (IEF) and DNA sequencing. With 400 W output, the PowerPac HV offers enough power to run the most demanding IEF experiments or up to four DNA sequencing cells simultaneously.

Optional wireless data transfer software and an IQ/OQ protocol binder and test box are also available.

Specifications

Output (programmable)	
Voltage	20–5,000 V
Current	0.01–500 mA
Power	1–400 W
Type of output (with automatic crossover)	Constant voltage, constant current, constant power, or constant temperature
Timer control	1 min to 99 hr, 59 min
Volt-hour control	Yes, 99,999 V-hr
Pause/resume function	Yes
Display functions	128 x 64 pixel, yellow-green backlit graphics LCD
Programmable methods	Stores up to 9 basic and 9 IEF methods, each with up to 9 steps
Real-time editing	Yes
Real-time clock	Yes
Automatic recovery after power failure	Yes, user-selectable; setup values maintained
Data transfer/archiving	Yes
Temperature control	Yes, via temperature probe; 30–90°C ± 2°C
Microampere readout and control	Yes
Safety features	No-load detection, sudden load change detection, ground leak detection, overload/short circuit protection, overvoltage protection
Operating conditions	0–40°C, 0–95% humidity
Stackable	Yes
Number of output jacks	4 sets in parallel
Regulatory	EN-61010, CE
IQ/OQ protocols	Yes
Input power (actual)	90–120 or 198–264 VAC, 50 or 60 Hz, autoswitching
Dimensions (W x D x H)	27.5 x 34 x 10 cm
Weight	2.85 kg (6.3 lb)

Minimum Hardware Requirements for Data Transfer Software

PC requirements	Windows XP or 2000 operating system
	400 MHz processor
	256 MB RAM minimum, 512 MB recommended
	1,024 x 768 pixel screen resolution with true-color mode (24 or 32 bits)
	6 GB hard drive
	CD-ROM drive
	IR port
PDA requirements	Palm OS software version 4.0 or 5.0
	8 MB memory

For more information, request bulletin 3189.

Ordering Information

Catalog #	Description
PowerPac HV Power Supply and Accessories, 100–120/220–240 V	
164-5056	PowerPac HV Power Supply, includes power cord, instructions
164-5059	PowerPac HV Power Supply With Temperature Probe
164-5097	PowerPac HV Data Transfer Software
164-5098	PowerPac HV IQ/OQ Protocol Binder and Test Box
164-5099	PowerPac HV IQ/OQ Protocol Binder

iScript™ Select cDNA Synthesis Kit

Reliable cDNA Synthesis Using Any First-Strand Priming Strategy

The iScript Select cDNA synthesis kit is the latest addition to the iScript reverse transcription product family. This flexible and sensitive cDNA synthesis kit provides a complete selection of priming approaches in a single kit. Its flexible format makes it suitable for a variety of applications, including RT-PCR, real-time RT-PCR, and the synthesis of cDNA fragments >6 kb in length for applications such as cloning.

Included in this kit are separate tubes of oligo(dT) and random primers. To improve first-strand synthesis, these primers are blended with a proprietary enhancer solution. For reactions using custom-designed gene-specific primers, a separate tube of enhancer solution is provided to ensure maximum sensitivity.

Unlike other reverse transcription kits with up to nine different reaction components that must be combined during reaction setup, the iScript Select cDNA synthesis kit features an optimized, preblended reaction mix containing all required components except primers, enzyme, and template. This preblended mix simplifies reaction setup, saves time, enhances reproducibility, and minimizes the risk of cross-contamination without compromising performance.

Key Features

- 3 different priming strategies, optimized for efficient cDNA synthesis and sensitive detection using 1 pg to 1 µg of input total RNA
- Quality controlled for reliable synthesis of cDNA >6 kb
- Optimized reaction mix preblended with dNTPs, an RNase inhibitor, and proprietary additives to give optimal results and maximum sensitivity
- Proven iScript™ RNase H+ MMLV reverse transcriptase for efficient cDNA synthesis

For more information, request bulletin 2894.

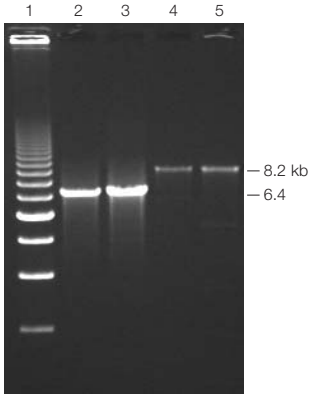

The iScript Select cDNA synthesis kit facilitates synthesis of cDNA longer than 6 kb. First-strand cDNA was produced from 1 µg total RNA using the iScript Select cDNA synthesis kit and the provided oligo(dT) primer mix. A 2 µl aliquot of the 20 µl cDNA synthesis reaction was subjected to 35 PCR cycles using a proofreading high-fidelity polymerase and human adenomatous polyposis coli (APC) primer sets. From a 50 µl PCR reaction, 10 µl was analyzed on a 1% agarose gel. Lane 1, 1 kb ladder; lanes 2 and 3, 6.4 kb APC PCR product; lanes 4 and 5, 8.2 kb APC PCR product.

Ordering Information

Catalog #	Description
170-8896	iScript Select cDNA Synthesis Kit, 25 reactions
170-8897	iScript Select cDNA Synthesis Kit, 100 reactions

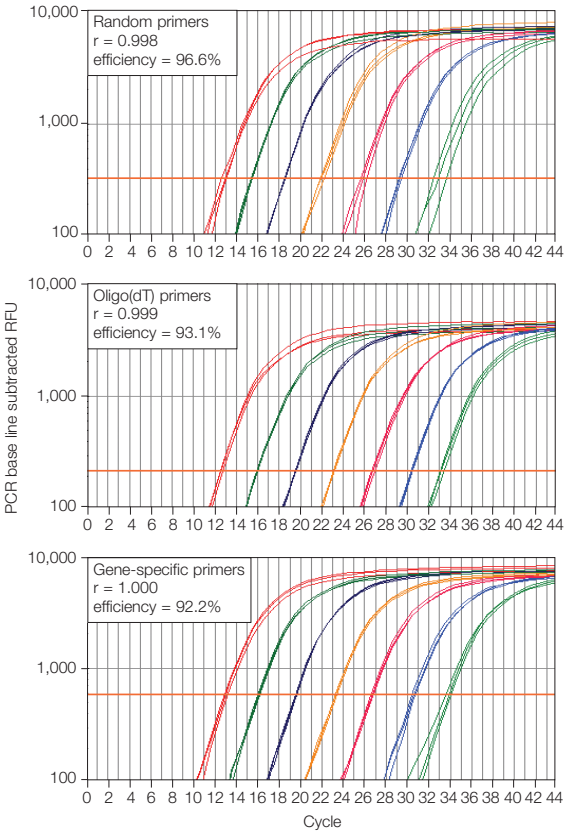

The iScript Select cDNA synthesis kit performs reliably over 6 orders of magnitude using any first-strand priming approach. Human total RNA from 1 pg to 1 µg was reverse transcribed using the iScript Select cDNA synthesis kit and the first-strand primers indicated above. The resulting cDNA was amplified in triplicate using iQ™ SYBR® Green supermix with β-actin primers and detected using the iCycler iQ® real-time detection system.

MJ Mini™ Gradient Thermal Cycler

Big Features in a Small Package

The compact yet powerful 48-well MJ Mini cycler boasts features found in larger instruments, including unparalleled thermal performance and MJ brand thermal gradient technology. A fully adjustable heated lid accommodates a variety of reaction vessels, and the 6 x 8 sample array accepts half-plates and tube strips. When fitted with the two-color MiniOpticon™ detector, this cycler can be transformed into the most compact real-time system available (see page 6).

Key Features

- Superior temperature performance that matches or exceeds high-performance 96-well thermal cyclers
- Real-time retrofit upgrade to the MiniOpticon real-time PCR system
- Thermal gradient of 1–16°C can be programmed along the sample block (front-to-back) for rapid optimization of reaction conditions in a single run
- Durable Peltier thermal electric modules for lasting performance
- Flexible capacity — 48 wells capable of fitting 12 x 0.5 ml tubes, 48 x 0.2 ml tubes, or a 48-well microplate without changing sample blocks
- High-performance cycling with options of block or calculated temperature control, auto-temperature increment, auto-time extend, and adjustable ramp rates
- Instant Temperature Incubate functionality sends the block to any temperature with just a few keystrokes
- Memory capacity for up to 400 standard programs
- Large 64 x 128 backlit semi-graphical display
- Power protection to resume programs after power outages

For more information, request bulletin 5262.

Ordering Information

Catalog #	Description
PTC-1148	MJ Mini Gradient Thermal Cycler With Adjustable Heated Lid, holds 48 x 0.2 ml tubes or 48-well microplate
MLL-4801	Multiplate™ Low-Profile 96-Well Unskirted PCR Plates, 8 x 6 format, natural, 50
TCS-0801	Domed 8-Cap Strips, for 0.2 ml tubes and plates, 130

Aurum™ Total RNA Fatty and Fibrous Tissue Kit

The Aurum total RNA fatty and fibrous tissue kit produces high yields of exceptionally pure total RNA from samples that are considered challenging. The kit is perfect for fatty and fibrous tissues or samples that are rich in RNases. It also works well with most animal and plant tissues, cultured cells, yeast, and bacteria. With this kit you can isolate up to 100 µg of total RNA — adequate for all sensitive downstream applications — from many sample types.

The Aurum total RNA fatty and fibrous tissue kit provides a quick, easy-to-follow procedure that combines the best features of one-step organic extraction with the speed and purity of silica-membrane purification. The kit includes sufficient reagents for 50 purifications of RNA from 5 to 100 mg of tissue or from only 50 up to 2.4 x 10^9 cells.

Key Benefits

- Optimal purification of up to 100 µg of high-quality total RNA from many sample types
- Exceptionally pure total RNA from samples in a spin-column format
- DNA- and phenol-free RNA suitable for most downstream applications, including real-time RT-PCR and microarray analysis
- RNase-free reagents and plasticware, including DNase I for removal of genomic DNA at no additional cost
- Quick preparation (<50 min without a DNase I digest step and 1.5 hr with a DNase I digest)

Ordering Information

Catalog #	Description
732-6830	Aurum Total RNA Fatty and Fibrous Tissue Kit, 50 preps, includes 50 ml PureZOL™ RNA isolation reagent, 50 RNA-binding mini columns, 50 capless collection tubes (2.0 ml), 100 capped microcentrifuge tubes (2.0 ml), 50 capped microcentrifuge tubes (1.5 ml), 1 vial lyophilized DNase I, RNase-free reagents and plasticware, protocol overview, instructions

MiniOpticon™ Real-Time PCR Detector

Big on Performance, Small on Size

The MiniOpticon system provides a compact, two-color real-time detection platform for the high-performance MJ Mini™ thermal cycler (see page 5). Together, they form the smallest and most portable system available for real-time PCR applications.

The MiniOpticon incorporates the same technology that drives the widely used Opticon™ 2 system — samples are illuminated sequentially by a fixed array of 48 blue-green light-emitting diodes (LEDs) to minimize cross talk. Emitted fluorescence is then detected by one of two filtered photodiodes. This innovative no-moving-parts design allows sensitive detection in a compact and robust package.

Key Features

- 2-color real-time PCR detection in a 48-well system
- A compact footprint (18 x 32 cm) allows the system to fit almost anywhere, and the system weighs just 6.8 kg
- The MJ Mini cycler base offers precise thermal control, and the temperature gradient simultaneously incubates samples at 8 different temperatures to optimize reaction conditions in a single run
- Ability to run up to 4 instruments from a single computer

For more information, request bulletin 5262.

Ordering Information

Catalog #	Description
CFB-3120	MiniOpticon Real-Time PCR System, includes optical housing and MJ Mini gradient thermal cycler
PTC-1148	MJ Mini Gradient Thermal Cycler With Adjustable Heated Lid, holds 48 x 0.2 ml tubes or 48-well microplate
CFO-3202	Optional Desktop Computer, 2.4 GHz processor, 256 MB RAM, 40 GB hard drive, 48 x 24 x 48 CD-RW, Windows XP Professional operating system (complete system requires OCM-3201)
OCM-3201	Optional 15" Flat-Screen Computer Monitor
CFO-3203	Optional Laptop Computer, 2.4 GHz processor, 256 MB RAM, 40 GB hard drive, 24 x 10 x 24 CD-RW, Windows XP Professional operating system
TLS-0851	Low-Profile 8-Tube Strips, 0.2 ml, white, 10 packs of 12 strips
TCS-0803	Optical Flat 8-Cap Strips, for 0.2 ml tubes and plates, ultraclear, 120
MLL-4851	Multiplate™ Low-Profile 48-Well Unskirted PCR Plates, white, 50

The iQ™5 Real-Time PCR Detection System

A New Generation for Real-Time PCR Analysis

The iQ5 real-time PCR detection system offers a fresh design for Bio-Rad's new generation of real-time PCR instrumentation. Like its predecessors, the iCycler iQ® and MyiQ™ systems, the iQ5 optical system is a modular upgrade to the iCycler® thermal cycler with 96-well reaction block. This powerful new system offers five-target analysis capabilities for multiplex PCR, coupled with a completely redesigned software package. The iQ5 optical system software offers a full suite of enhanced data collection and data analysis options, including new tools for gene expression analysis. Regardless of your PCR application, the iQ5 real-time PCR detection system is the ultimate system for value and flexibility.

Key Features

- Multiplexing of up to 5 fluorophores in each reaction vessel conserves precious samples and reagents
- Real-time PCR thermal gradient enables simple, rapid assay optimization
- Intuitive software for protocol setup and data analysis shortens time to results
- Diverse data analysis and presentation options provide a comprehensive view of your assay results
- Advanced gene expression analysis methods with publication-quality statistics and graphs for relative quantitation studies
- Flexible allelic discrimination module allows automatic sample identification in genotyping experiments
- Embedded tools for end-point fluorescence analysis enables simple qualitative assessment of sample abundance in single- or multicolor assays
- Robust, reliable thermal cycling performance delivered by the iCycler thermal cycler

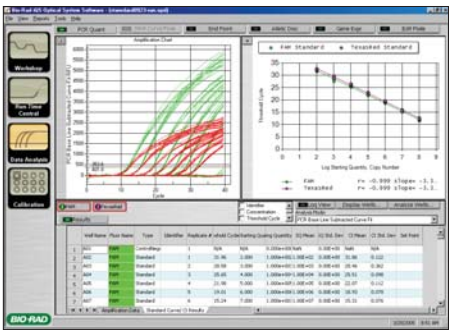

The iQ5 optical system software allows the display of amplification data and standard curves from all active fluorophores in a multiplex data set.

Perform relative sample quantitation without a standard curve using the Gene Expression analysis option in the iQ5 optical system software.

For more information on this and other real-time PCR systems, reagents, and accessories available from Bio-Rad, visit us on the Web at **www.bio-rad.com/amplification/**

Ordering Information

Catalog #	Description
170-9750	iQ5 Optical System, includes optics module, software CD-ROM, 5 installed filter sets, 96-well reaction module, calibration solutions, optical-quality 96-well PCR plates, communication cables, power cord, instructions
170-8701	iCycler Chassis, includes iCycler base, power cord, quick reference guide, instructions
223-9441	96-Well 0.2 ml Thin-Wall PCR Plates, 25

The right tool for those challenging samples

The Aurum™ total RNA fatty and fibrous tissue kit lets you focus on answering important scientific questions, instead of optimizing sample preparation.

- Quickly isolate up to 100 µg of high-quality total RNA from fatty or fibrous tissues or RNase-rich samples*
- Contaminant-free RNA is ready to use for downstream applications, including real-time RT-PCR and microarray analysis
- Easy-to-use protocol in a spin- or vacuum-compatible format
- Kit includes RNase-free reagents and plasticware, and DNase I for removal of genomic DNA

For a free trial size Aurum total RNA fatty and fibrous tissue kit, contact your local representative or visit us on the Web at **www.bio-rad.com/ad/fattyandfibrous/**

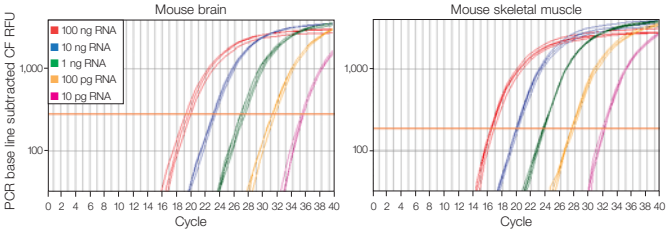

Excellent real-time RT-PCR results from RNA isolated using the Aurum total RNA fatty and fibrous tissue kit. Data acquired on the MyiQ™ system.

* Also compatible with most animal and plant tissues, cultured cells, yeast, and bacteria.

Visit us on the Web at **discover.bio-rad.com**
Call toll free at 1-800-4BIORAD (1-800-424-6723);
outside the US, contact your local sales office.

BIO-RAD

Accurate and Reproducible RNA Concentration Measurements Using the Experion™ Automated Electrophoresis System

Michael Urban, William Strong, and Christina Whitman-Guliaev
Bio-Rad Laboratories, Inc., 6000 James Watson Drive, Hercules, CA 94547 USA

Introduction

The assessment of RNA integrity and purity is an important first step to many gene expression analysis applications. It is preferable to use high-quality, intact RNA as a starting point for applications such as RT-PCR, ribonuclease protection assays, and northern analyses. In some cases, such as when performing cDNA library construction and microarray analyses, it is essential to qualify the RNA sample before moving forward because of the considerable time and expense involved. Additionally, the stability of RNA transcripts can differ widely throughout the cell, and RNA degradation during extraction and handling can bias the quantitation of transcripts in gene expression studies. Therefore, a system that provides both sample quality analysis and accurate quantitation adds confidence and value to the results of downstream applications.

The Experion automated electrophoresis system uses a combination of Caliper Life Sciences' innovative LabChip microfluidic separation technology and sensitive fluorescent sample detection to rapidly provide detailed information about RNA sample quality and concentration. Two Experion analysis kits are available for life science applications that require accurate, reproducible separation and detection of small volumes of total RNA or mRNA at nanogram and picogram levels. The Experion RNA StdSens (standard sensitivity) kit is designed for qualitative analysis and quantitation of 5–500 ng/µl total RNA and 25–250 ng/µl mRNA from eukaryotic or prokaryotic sources. The Experion RNA HighSens (high sensitivity) kit is used for qualitative analysis of 100–5,000 pg/µl total RNA and 250–5,000 pg/µl mRNA samples. The Experion system combines the utility and qualitative benefits of gel-based RNA analysis with the quantitative accuracy of spectroscopic analysis, although, unlike spectroscopic measurements based on UV absorbance, the Experion system shows no significant effects from residual phenol that is sometimes present in RNA samples (data not shown).

The Agilent 2100 bioanalyzer system is a related microfluidics-based electrophoresis system that uses the LabChip technology and assays that are functionally similar to the Experion system. In this report, we compare the performance of the Experion and 2100 bioanalyzer systems in analyzing both total RNA and mRNA samples. Included are a qualitative comparison of sensitivity for both systems and a comparison of the accuracy and reproducibility of RNA quantitation across the dynamic range for each system. The Experion system is demonstrated to improve performance by increasing sensitivity to offer more sample information. It also provides more accurate and reproducible quantitation of RNA samples, while allowing the use of smaller sample and reagent amounts.

Methods

Rat brain total RNA and mRNA samples and the 6000 RNA ladder were purchased from Ambion, Inc. Experion RNA HighSens and StdSens analysis kits were used for analysis with the Experion system. The RNA 6000 Nano and Pico LabChip kits were used with the 2100 bioanalyzer system and were obtained from Agilent Technologies.

RNA samples and ladders were prepared according to the protocols provided in the instruction manuals of the Experion RNA analysis kits and the Agilent RNA 6000 LabChip kits. RNA samples and ladders were first heat-denatured for 2 min at 70°C and then kept on ice until use. The heat-denatured total RNA and mRNA stocks were diluted to the desired final concentrations in either RNase-free TE buffer, pH 7.0 (for use with the Experion RNA StdSens and RNA 6000 Nano LabChip analysis kits) or in DEPC-treated water (for use with the Experion RNA HighSens and RNA 6000 Pico LabChip analysis kits).

Experion RNA chips were primed using the Experion priming station. The loading buffer was loaded into the wells, followed by the samples and Experion RNA ladder according to the kit protocol. The chip was then vortexed using the Experion vortex station and analyzed using the Experion automated electrophoresis station. The Agilent RNA chips were primed, loaded with loading buffer, samples, and ladder, vortexed, and analyzed using the Agilent manual priming station, vortexer, and 2100 bioanalyzer system, respectively, as described in the RNA 6000 Nano and Pico LabChip kit manuals. Each concentration of total RNA or mRNA was analyzed on both systems using a

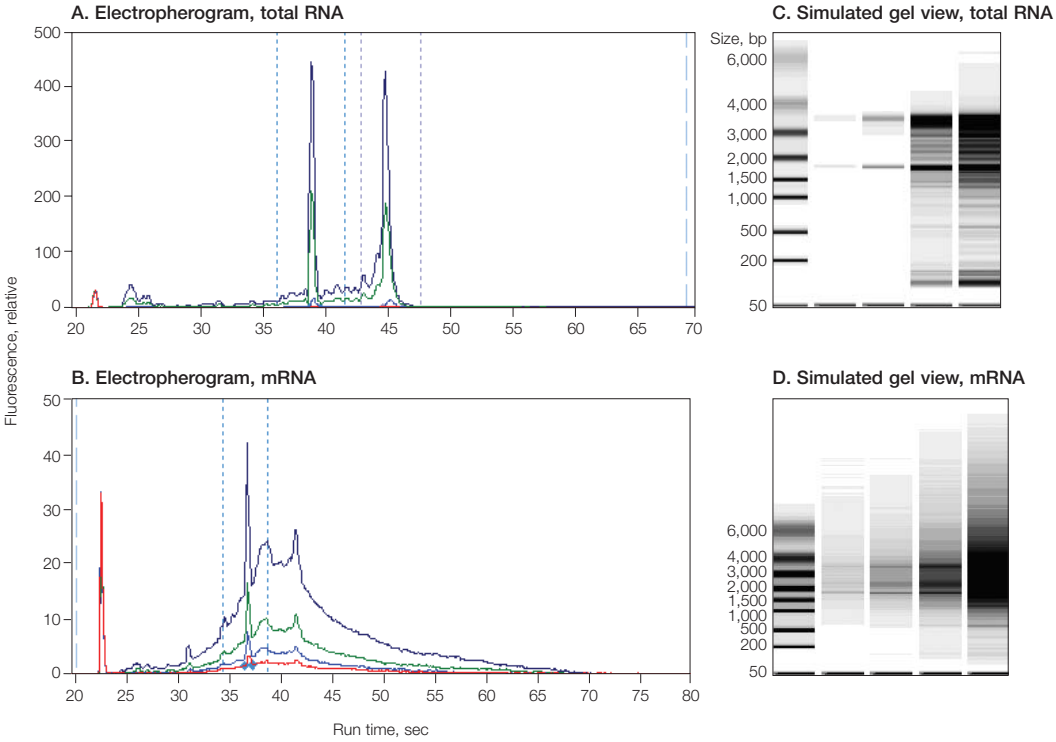

Fig. 1. Electropherogram (A, B) and simulated gel views (C, D) from an Experion eukaryotic RNA StdSens assay. Four samples of rat brain total RNA (5, 25, 100, and 500 ng/µl; A and C) and mRNA (25, 50, 100, and 250 ng/µl; B and D) were separated using the Experion RNA StdSens analysis kit. The Experion software's overlay function shows a direct comparison of the RNA integrity of multiple samples in the electropherograms. The simulated gel views also show the relative migration of the Experion ladder in the first well and the lower alignment marker (smallest band in each well).

minimum of five chips and three different wells per chip (n = 15 per concentration, per RNA type, except for the lowest concentration in the Experion RNA HighSens analyses, where n = 10).

Results and Discussion

Qualitative Performance

To minimize the variation in labeling efficiency for different sample preparations, both the Experion and bioanalyzer systems employ an RNA stain for detection that binds directly to the RNA moiety. Consequently, the fluorescence intensities of different sized fragments depend only on the RNA sample concentration and sensitivity of the detection method. Thus the differences in the fluorescence intensity measurements displayed in an electropherogram translate directly into differences in sample concentration. Both the Experion and bioanalyzer systems' software use fluorescence intensity measurements to calculate quantitative information, such as RNA concentration.

To determine the sensitivity and range of detection of both systems, identical preparations of rat brain total RNA and mRNA at several concentrations were analyzed using the Experion RNA StdSens and HighSens kits and the Agilent RNA 6000 Nano and Pico LabChip kits. The Experion RNA StdSens and Agilent RNA 6000 Nano LabChip kits were compared using four concentrations of total RNA within the analysis range for these kits (5–500 ng/µl) as well as four concentrations of mRNA (25–250 ng/µl). The Experion RNA HighSens and Agilent RNA 6000 Pico LabChip kits were compared using picogram levels of total RNA (100–5,000 pg/µl) and mRNA (250–5,000 pg/µl). The results from a typical analysis of the total RNA and mRNA concentration series using the Experion RNA StdSens analysis kit are shown in Figure 1.

A qualitative comparison of the electropherogram traces from identical total RNA and mRNA samples analyzed on each system revealed two general trends. First, both the Experion RNA HighSens and RNA 6000 Pico LabChip analyses correctly identified the ribosomal RNA peaks at all concentrations examined in the picogram concentration series (not shown), but only the Experion RNA StdSens analysis kit automatically identified the 18S ribosomal peak at the 5 ng/µl concentration of total RNA (Figure 2A and C). Second, the total fluorescent intensity from the 18S and 28S peaks in a given sample was, on average, approximately 4–5 times higher on the Experion system than on the bioanalyzer system. The improved detection with the Experion system facilitates reduced sample consumption. In addition, evaluation of the electropherogram for a sample of low concentration revealed that certain details of the RNA sample, such as the presence of small peaks in the 5S region (area between the lower marker and 18S RNA), were better resolved above the baseline when analyzed using the Experion system (Figure 2B and D). By providing additional sample information, such as the presence or absence of a peak or difference in the intensity of a fluorescence signal over the baseline in identical RNA samples, the Experion system demonstrates greater sensitivity than the bioanalyzer system.

Quantitative Performance

In addition to providing a quick visual assessment of RNA quality and integrity, through the display of the electropherogram view, the Experion software also performs sample quantitation (calculation of RNA concentration) and provides these results in the Results table. Knowing the sample quality and having accurate and reproducible quantitative data facilitates the successful planning and execution of downstream experiments, such as cDNA construction, microarray analysis, and RT-PCR analysis. The Experion software measures RNA concentration by calculating the total area under the electropherogram of an RNA sample and comparing it to that of the RNA ladder, which is provided in the Experion RNA analysis kits at a known concentration. Though the quality of the RNA ladder preparation and the consistency of chip preparation are important factors determining overall quantitation performance, this approach generally yields accurate and reproducible results. Because the Experion and bioanalyzer systems use similar methods for determining RNA sample concentrations, the accuracy and reproducibility of RNA quantitation with both systems may be directly compared.

To determine accuracy, the concentration of each RNA sample was analyzed with the Experion and bioanalyzer systems and then independently measured spectroscopically using UV absorbance at 260 nm. Accuracy, defined by the percent difference between the RNA concentration calculated by the Experion or bioanalyzer system (chip measurement) and that derived spectroscopically, was determined using the formula: [(software concentration – UV concentration)/UV concentration] * 100. Values close to zero indicate parity between the chip and spectroscopic measurements, and a negative or positive value indicates an underestimation or overestimation, respectively, of the chip measurement relative to the spectroscopic measurement.

The reproducibility of the Experion and bioanalyzer systems was evaluated using the coefficient of variation, or CV, as a statistical measure. For each RNA preparation tested, the CV of the concentration reported by the software was determined using the formula: [standard deviation/mean] * 100. CV was expressed as a percentage; small CV values indicate a small degree of variation in replicates and good quantitative reproducibility of the data. The results of the Experion and bioanalyzer data are summarized according to the type of RNA, concentration of RNA, and analysis kit used.

The data presented in Tables 1 and 2 represent the average measurement of the interchip (across multiple chips) accuracy and reproducibility for a given concentration and type of RNA. The data demonstrate that the Experion system provides better RNA quantitation accuracy than the bioanalyzer system. Whereas the Experion RNA StdSens kit displayed a maximum deviation from spectroscopic measurements for total RNA samples

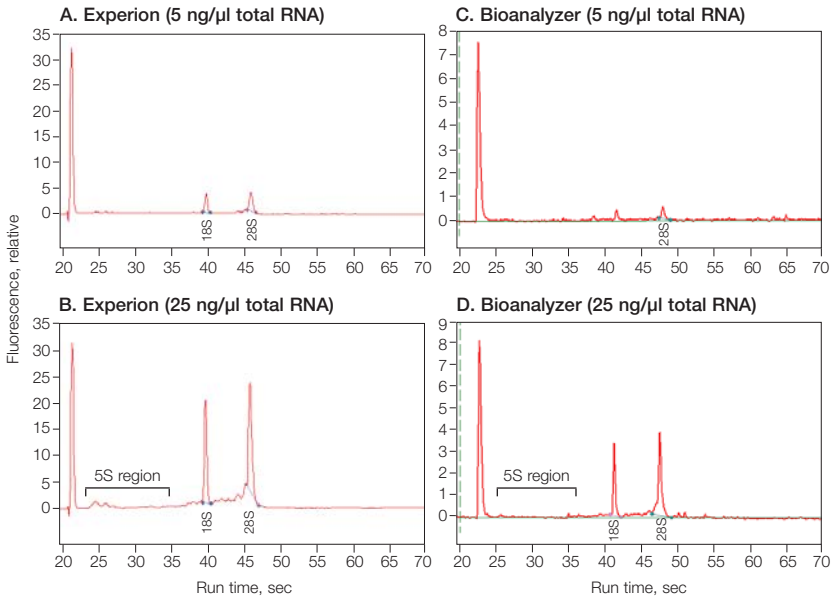

Fig. 2. Comparison of sensitivity. Electropherograms obtained from total RNA separations performed on the Experion (**A** and **B**) and Agilent 2100 bioanalyzer (**C** and **D**) systems using the nanogram analysis kits. The Experion system's greater sensitivity is shown by the higher fluorescent signal, which allowed improved sample detection. For 5 ng/µl total RNA, the 18S ribosomal RNA peak was automatically identified by the Experion system software (A), but not by the bioanalyzer system (C). For 25 ng/µl total RNA, the Experion system also resolved peaks in the 5S region, offering additional RNA sample information (B), while the bioanalyzer system did not provide the same level of detail (D).

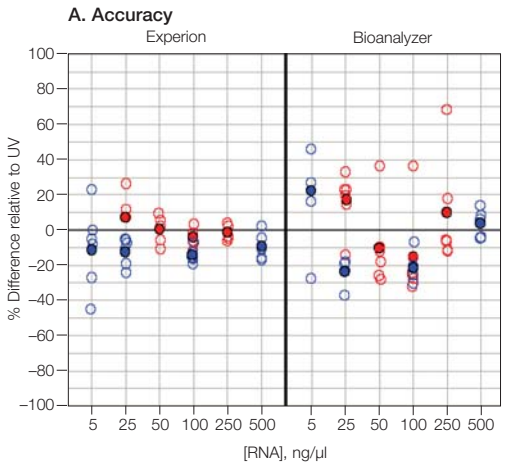

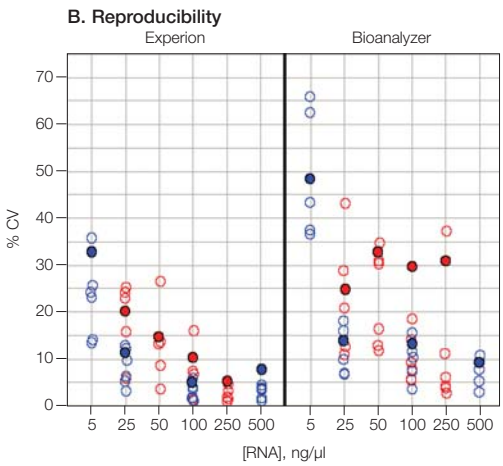

Fig. 3. Scatter plot comparison of quantitation accuracy (A) and reproducibility (B). Graphical representation of intrachip data (○, mRNA; ○, total RNA; average of 3 wells/chip) and interchip data (●, mRNA; ●, total RNA; average of 5 chips), also presented in Table 1. **Left panels**, data generated by the Experion RNA StdSens analysis kit; **right panels**, data generated by the RNA 6000 Nano LabChip kit.

Table 1. Comparison of accuracy* and reproducibility of quantitation of nanogram levels of RNA.** Total RNA and mRNA samples at the indicated concentrations were analyzed with the Experion RNA StdSens analysis kit and the RNA 6000 Nano LabChip kit using the Experion or Agilent 2100 bioanalyzer system, respectively.

	Experion		Bioanalyzer	
	Accuracy	Reproducibility	Accuracy	Reproducibility
Total RNA				
5 ng/µl	–10.7%	32.9%	21.6%	48.3%
25 ng/µl	–11.6%	11.6%	–24.1%	13.6%
100 ng/µl	–13.7%	5.3%	–20.6%	13.6%
500 ng/µl	–8.9%	7.9%	3.4%	9.0%
1,000 ng/µl***	3.4%	5.8%	—	—
mRNA				
25 ng/µl	7.5%	20.3%	17.0%	24.8%
50 ng/µl	0.4%	14.7%	–9.4%	33.0%
100 ng/µl	–4.6%	10.0%	–14.5%	30.0%
250 ng/µl	–1.7%	4.9%	10.0%	31.1%

* Calculated as % difference relative to values determined by UV.

** Calculated as % CV.

***The 1,000 ng/µl standard is outside the published concentration range for both the Experion and bioanalyzer systems, so the bioanalyzer system data is not included.

Table 2. Comparison of accuracy* and reproducibility of quantitation of picogram levels of RNA.** Total RNA and mRNA samples at the indicated concentrations were analyzed with the Experion RNA HighSens analysis kit and the RNA 6000 Pico LabChip kit using the Experion or Agilent 2100 bioanalyzer system, respectively.

	Experion		Bioanalyzer	
	Accuracy	Reproducibility	Accuracy	Reproducibility
Total RNA				
100 pg/µl***	—	9.1%	—	—
200 pg/µl	—	13.9%	—	17.0%
500 pg/µl	—	12.4%	—	10.2%
1,000 pg/µl	—	12.5%	—	26.1%
5,000 pg/µl	19.6%	9.4%	67.9%	9.4%
mRNA				
250 pg/µl***	—	17.6%	—	—
500 pg/µl	—	29.9%	—	19.7%
1,000 pg/µl	—	23.6%	—	19.1%
5,000 pg/µl	6.8%	33.4%	81.7%	22.4%

* Calculated as % difference relative to values determined by UV.

** Calculated as % CV.

***The Experion system has a published lower sensitivity range as low as 100 pg/µl (total RNA analysis) and 250 pg/µl (mRNA). The bioanalyzer system specifications are 200 pg/µl (total RNA) and 500 pg/µl (mRNA).

of 13.7%, the RNA 6000 Nano LabChip kit used with the bioanalyzer system produced up to 24.1% deviation for the same set of samples (Table 1). Similarly, the Experion RNA StdSens kit produced measurements within 7.5% of spectroscopic values for mRNA, compared to a maximum 17.0% deviation produced by the bioanalyzer system and the RNA 6000 Nano LabChip kit (Table 1). The quantitation accuracy of the Experion RNA HighSens kit and the RNA 6000 Pico LabChip kit was also examined at a single RNA concentration that could be independently measured by UV spectroscopy (5,000 pg/µl) using total RNA and mRNA samples. The overall percent difference between the spectroscopically measured concentration and that obtained using the Experion RNA HighSens kit was 19.6% for total RNA and 6.8% for mRNA, compared to 67.9% and 81.7% using the RNA 6000 Pico LabChip kit (Table 2). Taken together, these data demonstrate that the Experion system generally provides RNA concentration measurements that are most similar to those obtained by spectroscopic methods.

The data in Tables 1 and 2 also demonstrate that the Experion system displays greater reproducibility than the bioanalyzer system when used for RNA quantitation. Interchip CVs for the Experion RNA StdSens and HighSens kits ranged between 4.9 and 33.4%, while interchip CVs for the bioanalyzer system using the RNA 6000 Nano and Pico LabChip kits ranged between 9.0 and 48.3%. In addition, the reproducibility of both systems appeared to be higher for total RNA samples than for mRNA samples and tended to be the most precise at the higher concentrations of RNA that were tested. The total RNA and mRNA quantitation data generated using the bioanalyzer system and RNA 6000 Pico LabChip kit appear to be similar to those generated by the Experion RNA HighSens kit; however, it should be noted that the Agilent system consistently and significantly overestimated the concentration of the 5,000 pg/µl RNA preparations, as indicated by the accuracy data for these experiments (Table 2).

Additionally, Figure 3 presents the performance data for the RNA StdSens and RNA 6000 Nano LabChip kits graphically to illustrate both the interchip and intrachip (multiple wells within one chip) variations in the accuracy and reproducibility. The distribution of data points in Figure 3 clearly illustrates that the overall chip-to-chip variation for both accuracy (Figure 3A) and reproducibility (Figure 3B) measurements is much smaller for the Experion system regardless of the type of RNA.

Conclusions

The Experion system demonstrates improved performance over another commercially available system based on LabChip microfluidic separation technology. The Experion system's greater sensitivity of detection provides the capability to automatically acquire additional sample information, such as the presence or absence of a peak or peak variations in identical samples, for better qualitative assessment of RNA samples. Overall, the Experion system provides RNA concentration measurements that are more accurate, as they are most similar to those obtained by the traditional spectroscopic methods, while consuming smaller amounts of sample and reagents. The Experion system also displays better reproducibility in RNA sample quantitation, as illustrated by the observed small variations in both interchip and intrachip CV values.

The Experion system combines two valuable sample assessments, qualitative and quantitative, into a single analytical process, and provides higher sensitivity, better quantitation accuracy, and greater reproducibility for both total RNA and mRNA samples.

For more information on the Experion system, see BioRadiations 115 (p 16–21) or request bulletin 5285.

CHT™ Ceramic Hydroxyapatite, 40 µm — Optimized Packing Method in GelTec™ Columns

Larry Cummings, Bio-Rad Laboratories, Inc., Hercules, CA 94547 USA and Pierre Vidalinc, Bio-Rad Laboratories, Riom, France

Introduction

Most traditional chromatography columns for bioprocessing have been developed for use with polymer- or agarose-based resins with densities in the range of 0.40 to 0.65 g/ml and slow settling velocities. New columns, such as GelTec columns, include design features that accommodate heavier media based on inorganic materials, such as ceramic hydroxyapatites or silicas with fast settling velocities. These new design features allow easier packing and unpacking of materials with densities in the extended range of 0.35 to 1.3 g/ml.

CHT ceramic hydroxyapatite has a bulk density of 0.63 g/ml and a free-settling velocity of 0.075–0.125 cm/sec. The range of the settling velocity is due to the smallest and largest particles in the product, 20 and 60 µm. The rapid free-settling velocity is the primary reason for difficulty in packing uniform beds of CHT.

Fixed contained operating systems are packed more easily than open columns. Open columns, although more difficult to pack, are manageable if the column is level and inert gas is used to maintain the suspension. Bio-Rad's GelTec columns, which are contained operating systems, are filled with media in suspension through filling ports. The upper frit assembly is easily lowered to mate with the packed medium, since the assembly is already in place. This allows the operator to easily flow-pack or to axially compress the medium.

Column unpacking of high-density media can be challenging. Contained operating systems use nozzles to loosen the medium at the base of the column, creating a thick suspension. This suspension is pumped out of the column to a receiving reservoir.

Most columns on the market require 10 column volumes (CV) of unpacking buffer to completely remove higher-density media. GelTec columns can be unpacked in ≤5 CV due to the unique inlet valves that allow higher flow rates.

Fig. 1. GelTec 45 cm ID column that is being primed, sanitized, and rinsed.

Methods

The packing buffer, 0.2 M sodium phosphate, pH 7.0, was prepared by dissolving disodium hydrogen phosphate and sodium dihydrogen phosphate salts in 400 L water for injection (WFI). Test buffer (0.15 M NaCl/20 mM sodium phosphate, pH 7.2) was prepared by adding 40 L Bio-Rad 10x PBS to 360 L WFI.

CHT Type I, 40 µm, Bio-Rad lot M400225, which had been stored in 0.1 M NaOH for approximately 1 year, was examined microscopically to ensure particle integrity. Fines and broken particles were not observed. The NaOH supernatant was decanted, the CHT was suspended in an equivalent volume of WFI and allowed to settle, then the remaining supernatant was decanted. The CHT was then suspended in an equivalent volume of packing buffer and allowed to settle, then the packing buffer was decanted.

A 45 cm inner diameter (ID) GelTec column was prepared for packing (Figure 1). The upper frit assembly was raised to its maximum height, leaving a distance of 54 cm between the surfaces of the upper and lower frit assemblies (approximately 84 L). A sufficient amount of CHT was poured into the slurry transfer reservoir to make 75 L of a 40%

Fig. 2. GelTec column filled with CHT suspension.

Fig. 3. CHT packed to 17.8 cm.

(v/v) slurry in packing buffer. The suspension was maintained with adequate mixing to ensure a homogeneous suspension.

The slurry was transferred to the column through the filling ports without regard to air bubbles introduced when the slurry tank emptied. The wall of the slurry tank was rinsed with two 2.5 L aliquots of packing buffer, which were then transferred to the column.

The filling ports were closed and the CHT was allowed to settle briefly to establish a buffer layer approximately 3 cm high above the bed. The upper frit assembly was lowered into the buffer, air bubbles were removed by shaking the anti-torsion bar, and the seal was inflated to 4 bar. The frit assembly was lowered at 120 Hz (220 cm/hr, Figure 2). About 2 min after beginning to lower the upper frit assembly, the total flow rate was increased by turning on the pump. The combined flow rate was approximately 370 cm/hr. The pressure was 2.5 bar.

The motor to the upper frit assembly was shut off when the frit compressed slightly into the packed bed of CHT. The safety feature on the packing skid indicated a change in power requirement, signaling completion of the axial packing step. The final bed height was 17.8 cm (Figure 3).

The column was equilibrated with 3 CV of running buffer at 150 cm/hr, the UV monitor was zeroed, and the BioLogic™ HR method was set to start mode. The bubble trap was bypassed, then 670 ml (approximately 2–2.5% CV) of test solution (1.75 M NaCl/2% acetone) was injected through port B of the pump inlet selector valve. The BioLogic HR program was started to obtain real-time data. After the sample cleared the injection line (1 min), the bubble trap was engaged to dampen pump pulsation.

Height equivalent to theoretical plate (HETP), asymmetry factor (A_f), and plates/m (N) were determined by inputting the times for maximum peak height, 50% peak height, 10% peak height, and column height. The test fixture is shown in Figure 4.

For unpacking, the column was equilibrated with 3 CV WFI to remove phosphate buffer and salt. The inflatable seal was partially deflated, then the upper frit assembly was raised at 220 cm/hr (120 Hz) while simultaneously flowing WFI into the column outlet at 220 cm/hr. The CHT bed rose at the same rate as the upper frit assembly. The process was stopped when the assembly reached 35 cm above the bottom frit assembly. The flow

Fig. 4. Test fixture.

was reversed for 1 CV of WFI to cause the bed to collapse, then switched to upflow for 1 CV. The bed lifted and peeled away from the column wall (Figure 5). The lower chamber of the column was opened to allow the collapsed CHT to enter the evacuation chamber. The slurry-transfer skid was turned on to remove the thick slurry from the chamber to the slurry reservoir. Approximately 0.25 CV of WFI was sprayed into the column to suspend the remaining CHT, then pumped out from the lower chamber (Figure 6).

Results

Target HETP values are unknown in process columns because of the vast differences in column design. After packing was optimized for the GelTec column, we obtained results for both the UV and conductivity traces. For the UV trace, HETP = 0.016 cm, A_f = 1.29, and N = 6,352. For the conductivity trace, HETP = 0.016 cm, A_f = 1.22, and N = 6,260.

Conclusions

A very efficiently packed chromatographic bed of CHT ceramic hydroxyapatite was achieved with a GelTec column using a combination of flow-packing and axial-compression packing, and a minimum of packing buffer. The column was also easy to unpack, requiring only 3–5 CV of liquid to empty the column.

For copies of a similar article, request bulletin 3199.

Fig. 5. Collapsed CHT bed.

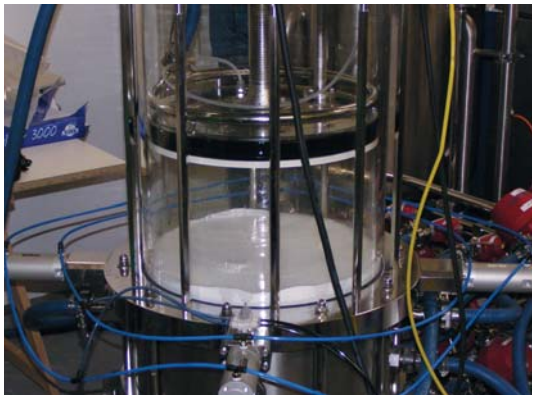

Fig. 6. Emptying of lower chamber.

RNAi:

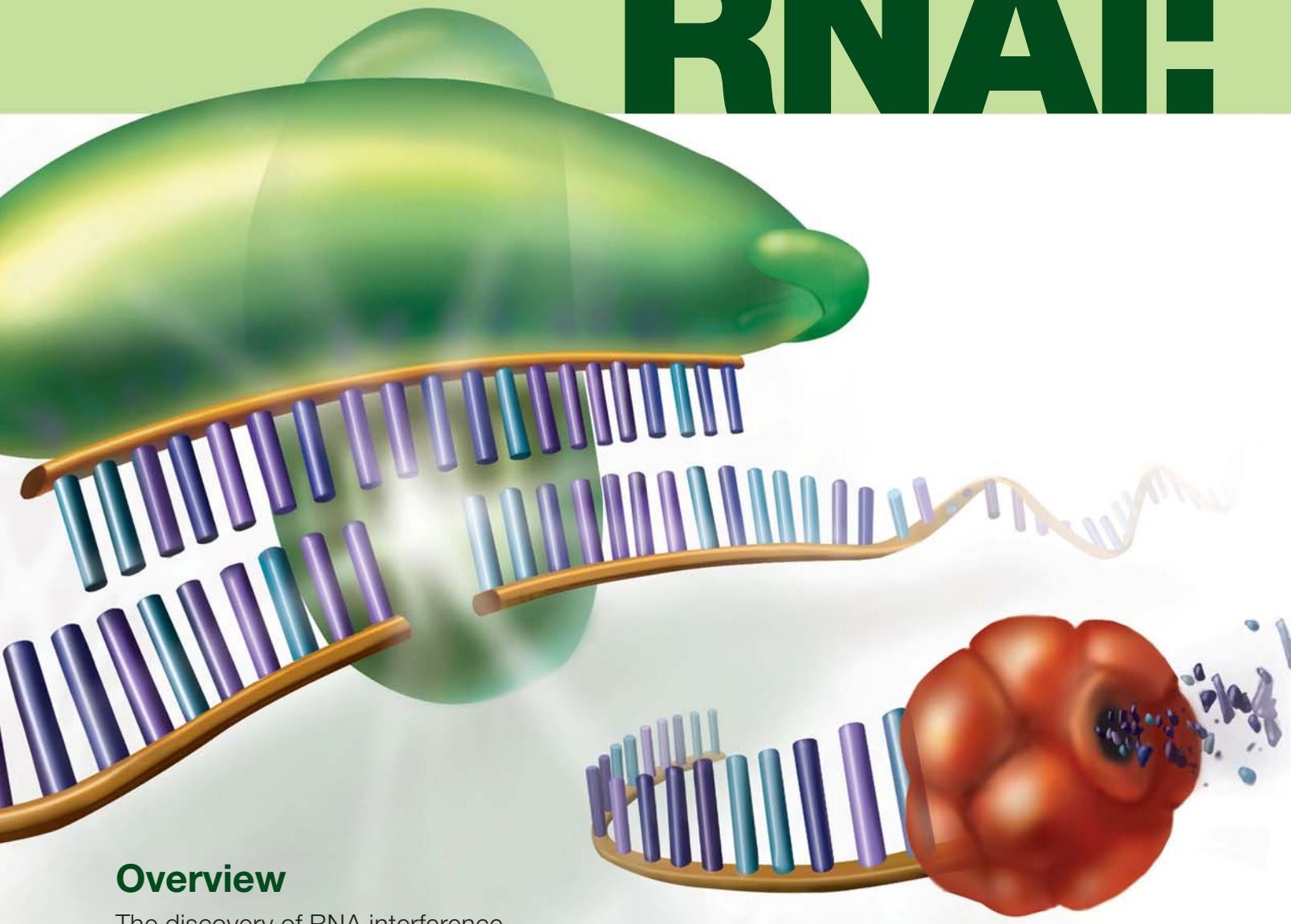

Overview

The discovery of RNA interference (RNAi) has significantly benefited the ability to modulate gene expression and investigate gene function.

RNAi is a naturally occurring pathway activated by a double-stranded RNA. Homology between this double-stranded small interfering RNA (siRNA) and an mRNA expressed by the cell leads to a reduction in the level of the mRNA. RNAi appears to be well conserved throughout evolution, having been identified in a number of organisms. While the mechanism of RNAi varies across different species, all manifestations ultimately have in common the use of siRNAs, 21–23 nucleotides in length, to stimulate sequence-specific degradation of homologous messenger RNA transcripts (Fire et al. 1998, Elbashir et al. 2001).

Delivery to Detection

Authors: Julie Moore, Nebila Idris, and Hilary Srere, Bio-Rad Laboratories, Inc., Hercules, CA 94547 USA

RNAi can be used as an experimental tool to interfere with gene expression by the introduction of siRNAs into cells through gene knockdown experiments. Although the RNAi field is still young, the use of RNAi has already been demonstrated to have great potential for understanding gene function, elucidating biological pathways, and identifying and validating potential drug targets (reviewed in Hannon and Rossi 2004, Mello and Conte 2004).

Since RNAi is ultimately mediated by siRNAs, scientists performing RNAi experiments in mammalian systems must first deliver siRNAs into cells. siRNA can be produced in vitro through a number of methods, including chemical synthesis, in vitro transcription, and RNase III digestion of long dsRNA. Alternatively, siRNAs can be generated inside the cell using vector-based siRNA transcription systems. These can take the form of a linear siRNA expression cassette (SEC) or a circularized plasmid containing a cloned sequence under the control of an H1 or U6 Pol III promoter. Once inside the cell, transcription of these cloned sequences yields dsRNA, usually in the form of a short hairpin loop (shRNA). This is then processed by Dicer, a member of the RNase III family, into functional siRNAs (Bernstein et al. 2001, Nykanen et al. 2001, Meister and Tuschl 2004).

The siRNAs form a complex with an RNA-protein complex called RISC, the RNA-induced silencing complex, which mediates the detection and subsequent degradation of mRNA containing the same sequence (reviewed in Hannon and Rossi 2004).

Following delivery of siRNAs to the cell, suitable sample preparation and analysis methods are required to verify the effectiveness of degradation of the target mRNA. Although newer siRNA design algorithms have a high rate of success (Khvorova et al. 2003, Schwarz et al. 2003), the possibility of failure still remains. To assess the effectiveness of the inhibition, researchers can examine the levels of either the target gene or the corresponding protein to determine whether they have been reduced. Although western blots are still commonly used, and are important for the detection of protein, reverse transcription followed by quantitative PCR provides a quick and effective method for measuring the reduction in mRNA transcript. Below we discuss important aspects of delivery, sample preparation, and validation of knockdown using real-time reverse transcription quantitative PCR (RT-qPCR).

Illustration by Megan Rojas

Optimizing Delivery of siRNA Using Lipid Transfection

One step critical to the success of any siRNA-mediated downregulation in mammalian cells is the efficient delivery if the siRNA into cells. There are a number of methods available, including lipid transfection, electroporation, biolistic particle delivery, microinjection, and viral vector systems. The method chosen depends on its effectiveness for the cell type being used. For most mammalian cell cultures, lipid transfection is a popular method due to its efficiency, ease of use, low cost, and adaptability to high-throughput systems.

Here, we discuss the characteristics of lipid transfection reagents that are important for effective delivery and present data that demonstrate the value of this optimization.

Choice of Transfection Reagent

As mentioned above, a number of approaches can be used to introduce siRNA into cells. While the introduction of synthesized siRNA often results in greater knockdown, vector-based systems have the advantage of longer-lasting silencing due to their inherent cellular stability and their ability to make multiple copies of shRNA, resulting in slower dilution of the active molecules.

Each approach requires effective transfection, and thus the specific molecules used as the source of siRNA — small dsRNA molecules or the larger DNA vector systems — will influence the selection of the most suitable lipid. Bio-Rad offers two lipids with characteristics that make them excellent choices for RNAi applications (Table 1).

Table 1. Bio-Rad's transfection reagents suitable for RNAi experiments.

Source of siRNA	Lipid Reagent
siRNA • Chemically synthesized siRNA • In vitro transcribed siRNA • Dicer/RNase III siRNA cocktail	**siLentFect**
DNA • Expression vector (cellular) • Expression cassette (SEC)	**TransFectin**

siRNA Delivery

TransFectin™ and siLentFect™ Reagents

RNA Sample Preparation

Aurum™ RNA Kits

Experion™ System

RT-qPCR

iScript™ cDNA Synthesis Kit

iCycler iQ® System

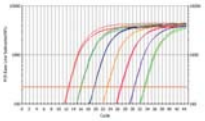

siLentFect lipid reagent for RNAi is a high-efficiency cationic lipid developed for in vitro delivery of siRNA, and TransFectin lipid reagent was developed for the introduction of dsDNA across a broad range of mammalian cells.

Regardless of the method used for mediating RNAi, transfection should be carefully optimized for each cell line used. Factors to consider include the quality and quantity of siRNA used, the confluency of cells at transfection, the passage number, and the medium composition.

Efficiency of of Nucleic Acid Delivery

Efficiency of delivery refers to the lipid reagent's ability to deliver nucleic acid to the cell. This is primarily a function of the lipid's stability as a complex and its ability to effectively interact with the cell membrane. For RNAi, successful delivery to as many cells as possible is important, since reduction in expression can be measured by background expression from untransfected or control cells (Figure 1).

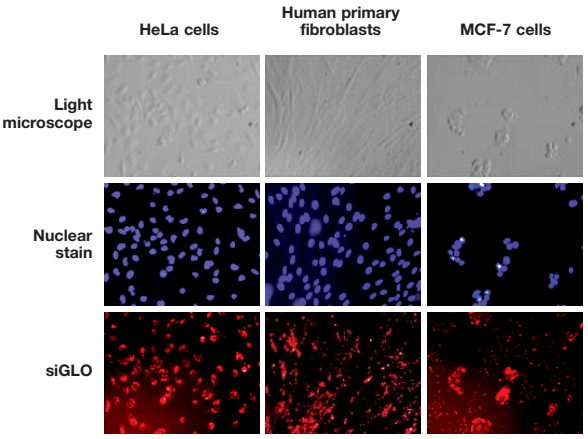

Fig. 1. Efficient intracellular delivery of siRNA by siLentFect. To directly assess the efficiency of transfection, a modified siRNA containing a fluorescent label (siGLO, Dharmacon) was used. Cells in a 24-well plate were transfected with 10 nM siGLO siRNA (red) and 0.5 µl of siLentFect. After 24 hr, cells were stained with a nucleus-specific stain, Hoechst 33342 dye (blue), and examined by fluorescence microscopy. The images show both the perinuclear and cytoplasmic localization of the fluorescent siRNA, and the uniform uptake of the siGLO siRNA by all cultures.

Avoiding Off-Target Effects

There have been many reports on the effects of siRNAs in initiating "off-target" effects in mammalian cells — the inhibition of genes that were not targeted. While some reports indicate no significant changes in the expression levels of untargeted transcripts (Chi et al. 2003), others have demonstrated significant changes (Jackson and Linsley 2004, Jackson et al. 2003). In some cases, the changes observed seem dose dependent, with increased off-target or nonspecific effects resulting from an increased level of delivered siRNA (Persengiev et al. 2004). In these cases, a lipid that complexes with siRNA efficiently will enable lower doses to be delivered, while still producing effective knockdown of the targeted gene (Figure 2).

Minimizing Cell Toxicity

Ensuring that a lipid reagent exhibits low toxicity at the optimal concentration is important. Results of a knockdown can be biased by cell death. Unless proper controls are run, it can be difficult to recognize how much knockdown (as measured by transcript reduction) is due to the siRNA and how much is the result of global transcriptional arrest and cell death. In addition to visually monitoring the cells to ensure they appear healthy, a titration of lipid volume should be performed to determine the optimal volume needed, since too little lipid results in inefficient transfection and too much can be cytotoxic. An example is shown in Figure 3. The control showed no reduction in activity — even at higher volumes of lipid — indicating no toxicity at these levels. The test culture showed a specific reduction in reporter gene activity. The difference between the test and control is a good indication of the quality of data.

Protocol Flexibility

In addition to efficient siRNA transfection with low cytotoxicity, a good transfection reagent should reliably deliver high performance among multiple wells for replicate samples and different lots of the transfection reagent. Such characteristics are especially important in high-throughput screening of siRNA libraries. Some high-throughput laboratories have adopted a reverse transfection method, developed by Ziauddin and Sabatini (2001), in which siRNAs are spotted on the bottom of wells or on glass slides. Cells are overlaid and transfection occurs over the siRNA spot, enabling phenotypic analysis. siLentFect allows successful application of this technique (data not shown).

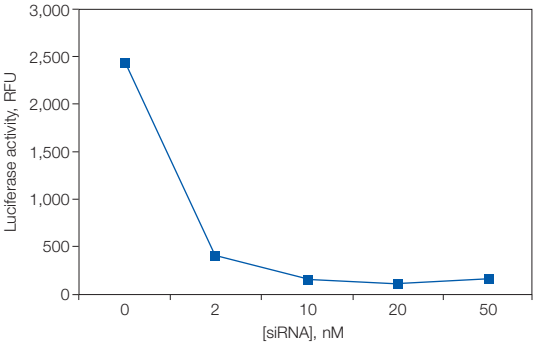

Fig. 2. Luciferase knockdown with low doses of siRNA. CHO-Luc cells stably expressing the luciferase gene were transfected in 96-well plates using 0.3 ml of siLentFect and different concentrations (2–50 nM) of anti-luciferase siRNA. At 48 hr after transfection, cells were harvested and luciferase expression was analyzed. The luciferase gene was downregulated >80% with only 2 nM siRNA, and >90% at 10 nM siRNA. The addition of >10 nM siRNA did not reduce luciferase activity further. siLentFect has a very high affinity for siRNA, resulting in a high molar efficiency; therefore, low concentrations of siRNA are sufficient for efficient silencing.

Cotransfection of siRNA and Plasmid DNA

When testing siRNAs, a common protocol setup is to cotransfect a plasmid expressing the gene of interest along with an siRNA to knock down the transcript of that gene (Figure 4). A control culture is cotransfected with a plasmid expressing luciferase and a nonspecific (control) siRNA to demonstrate expression from the plasmid. In the test culture, the same plasmid is delivered together with the test siRNA (Figure 4).

Sample Preparation for RNAi Validation

Need for High-Quality RNA

Obtaining high-quality RNA is a critical requirement for RNAi experiments. RNA isolation has been traditionally viewed as challenging, primarily due to the ubiquitous presence of stable RNases, which can easily degrade RNA samples. Sample preparation is also important to ensure absence of contaminants that can affect downstream results, such as PCR inhibitors or genomic DNA when RT-PCR-based message detection is used. If a DNase step is used to degrade genomic DNA, residual DNase must also be removed.

Aurum total RNA kits isolate highly pure RNA that meet these requirements. These kits are efficient and easy-to-use, and are available in spin- or vacuum-compatible formats to streamline sample preparation. Because cell lysis is a critical step in RNA extraction, Aurum total RNA kits are provided with a lysis solution that inhibits endogenous RNases, preventing RNA degradation. Cell lysates are loaded onto silica membranes in a column or 96-well format under conditions that promote selective binding of RNA to the membranes. Removal of residual genomic DNA is performed quickly using an on-column or in-well treatment with a high-quality DNase I (supplied with the kits). Subsequent wash steps effectively remove residual DNase. Once eluted, the RNA is ready for downstream applications — without the need for further manipulation, such as ethanol precipitation.

Once total RNA has been isolated, its quality should be assessed before analyzing gene expression. Traditionally, this is done by assessing the absorbance of the sample at 260 nm, followed by resolving an aliquot on a denaturing agarose gel and staining it with ethidium bromide in order to determine sample integrity. An alternative method that uses microfluidics and automated electrophoresis to simultaneously quantitate and assess the quality of an RNA sample is Bio-Rad's recently introduced Experion automated electrophoresis system (see page 9).

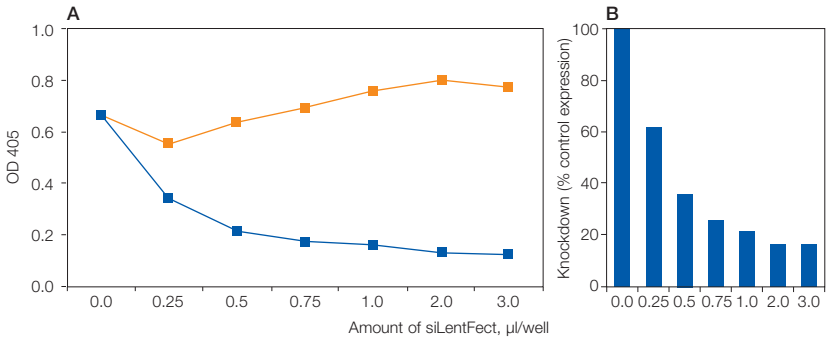

Fig. 3. β-Galactosidase knockdown, illustrating targeted reduction in reporter gene activity with minimal toxicity. Stable CHO-*lacZ* cells were transfected in 24-well plates with 10 nM anti-β-galactosidase siRNA (■) or nonspecific control siRNA (■) using siLentFect. **A**, assay for β-galactosidase activity at 24 hr; **B**, knockdown (ratio of anti-β-galactosidase to control values). The control showed no reduction in activity even at higher volumes of lipid, confirming that the reduction in reporter gene activity was due to siRNA knockdown.

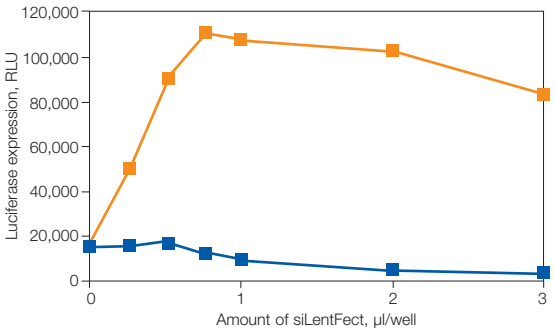

Fig. 4. Cotransfection of siRNA and plasmid DNA. MCF-7 cells were transiently transfected in 24-well plates with different volumes of siLentFect, 0.5 µg of a luciferase reporter gene expression vector, and 10 nM of either a nonspecific siRNA control (■) or an anti-luciferase siRNA (■). siLentFect was allowed to complex first with the siRNAs and then with the plasmid. After 20 min, the complexes were added to the cells. Luciferase activity was measured 24 hr posttransfection. This experiment shows that siLentFect may be used to deliver both plasmid and siRNA to cells to achieve silencing of a gene expressed by a cotransfected plasmid.

Validation of siRNA-Mediated Knockdown Using qPCR

Real-time RT-qPCR has become the accepted tool for validation of many different techniques, including microarray analysis, gene transfer, and knockdown and knockout experiments. This is because the researcher can obtain accurate and sensitive quantitative results with a well-designed RT-qPCR assay. In siRNA knockdown experiments, RT-qPCR is used to verify that the mRNA for the targeted gene has in fact been downregulated.

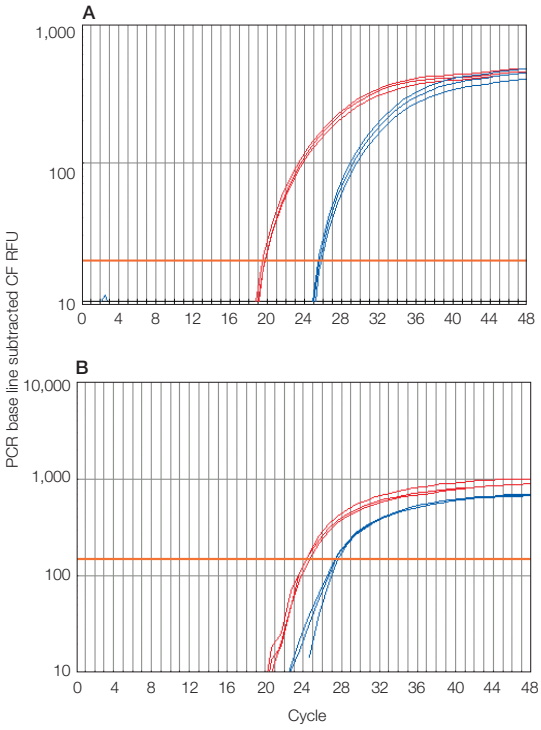

Fig. 5. Endogenous gene downregulation. Expression of an endogenous gene target, GAPDH, in HeLa (**A**) and MCF-7 cells (**B**). Cells were transfected in 6-well plates with 2 µl of siLentFect and 10 nM nonspecific control siRNA (—) or a GAPDH *SMART*pool siRNA (—) (Dharmacon). Cells were harvested at 48 hr posttransfection, and RNA was isolated using the Aurum total RNA mini kit. cDNA was produced using the iScript cDNA synthesis kit and RT-qPCR performed using the iCycler iQ real-time PCR detection system.

To achieve the best performance in RT-qPCR assays, four aspects of the assay must be optimized: sample preparation, the reverse transcription system, primer and probe design, and primer and probe performance (see sidebar).

Table 2. Relationship between differences in C_T values and gene silencing (knockdown).

ΔC_T	% Knockdown
1	50%
2	75%
3.3	90%
6.6	99%

Once an optimized assay for the target genes has been designed, confirming the effect of siRNA treatment on the cells is simple. Figures 5 and 6 show examples of experiments in which qPCR was used to verify the effectiveness of RNAi. In the experiment shown in Figure 5, endogenous mRNAs were silenced in HeLa and MCF-7 cells. These two cell lines were treated either with siRNA targeted against glyceraldehyde-3-phosphate dehydrogenase (GAPDH) or with a nonspecific control siRNA. At 48 hr after transfection, total RNA was isolated, then reverse transcribed, and the resulting cDNA was used in a qPCR reaction. By simply comparing the threshold cycle (C_T) of each reaction (specific vs. control siRNA), the level of mRNA silencing can be determined (Table 2). The results in Figure 5 show that the reaction involving the specific siRNA had a C_T value 3.8 cycles later than the C_T of the control reaction, indicating a >90% reduction of the GAPDH message in both cell lines.

Figure 6 shows changes in expression of genes in the polyamine biosynthesis pathway following treatment of human primary fibroblasts with

Optimizing RT-qPCR Assays

Sample Preparation

As with all techniques, sample purity is important in RT-qPCR. To generate reliable RT-qPCR data, the sample material used for RNA preparation should be as homogeneous as possible. Using tissue-culture cells is generally advantageous because most cultured cells are inherently homogeneous. For general advice on obtaining high-quality DNA that lacks inhibitors of PCR, refer to the recommendations on page 19.

Reverse Transcription

The reverse transcription step is critical for accurate quantitation of the sample material. The amount of cDNA synthesized in the RT reaction should accurately represent the input RNA population, which requires a reverse transcriptase with appropriate sensitivity, specificity, and dynamic range.

Primer and Probe Design

For most real-time applications, the primer pairs are designed to generate PCR products that are 60–200 bp long. Short PCR products are preferred.

Primer and Probe Performance

It is crucial that primer pairs amplify their target sequences with the highest efficiency possible (>90%). To measure the performance of primer and probes, a serial dilution of the templates is prepared and these dilutions are amplified using PCR. The results can be used to calculate the efficiency of the reaction. A 3.3-cycle delay (with the C_T of the specific reaction being 3.3 cycles later than that of the control) corresponds to a 90% knockdown of message level in the original sample. A 6.6-cycle delay corresponds to a 99% knockdown.

Once an optimized assay has been developed, using RT-qPCR to confirm the efficacy of siRNA-mediated knockdown in samples is a straightforward method capable of determining the mRNA levels of several genes (up to four) across many samples (up to 96) in a single assay.

For more information and a step-by-step description of how to optimize qPCR assays, refer to Persson and Ugozzoli (2004) in BioRadiations 113.

difluoromethylornithine (DFMO) or an siRNA specific to the ornithine decarboxylase (ODC) transcript. ODC activity is inhibited in the presence of DFMO, resulting in reduced polyamine levels and a subsequent decrease or arrest in cell division. DFMO inhibits the protein, whereas the siRNA targets the mRNA. As expected, the qPCR results showed no change in the ODC transcript level following DFMO treatment, but a downregulation of >99% with siRNA treatment (Figure 6A). Interestingly, the message level of another gene in this pathway was upregulated following both DFMO and anti-ODC siRNA treatment (Figure 6B). The last two genes in the pathway studied showed no change in transcript level with either treatment (Figure 6C and D).

Conclusions

With the proper approach and tools, RNAi experiments allow knockdown of target gene expression, enabling a better understanding of gene function. To successfully use RNAi, an awareness of the means of siRNA delivery, as well as sample preparation and validation techniques to enable detection of target gene levels, is essential. To facilitate the approach, Bio-Rad offers a variety of tools for each step in the process — from delivery to detection — of evaluating the effectiveness of such knockdown experiments.

References

Bernstein E et al., Role for a bidentate ribonuclease in the initiation step of RNA interference, Nature 409, 363–366 (2001)

Chi JT et al., Genome wide view of gene silencing by small interfering RNAs, Proc Natl Acad Sci USA 100, 6343–6346 (2003)

Elbashir SM et al., RNA interference is mediated by 21- and 22-nucleotide RNAs, Genes Dev 15, 188–200 (2001)

Fire A et al., Potent and specific genetic interference by double-stranded RNA in *Caenorhabditis elegans*, Nature 391, 806–811 (1998)

Hannon GJ and Rossi JJ, Unlocking the potential of the human genome with RNA interference, Nature 431, 371–378 (2004)

Jackson AL and Linsley PS, Noise amidst the silence: off-target effects of siRNAs?, Trends Genet 20, 521–524 (2004)

Jackson AL et al., Expression profiling reveals off-target gene regulation by RNAi, Nat Biotechnol 21, 635–637 (2003)

Khvorova A et al., Functional siRNAs and miRNAs exhibit strand bias, Cell 115, 209–216 (2003)

Meister G and Tuschl T, Mechanisms of gene silencing by double-stranded RNA, Nature 431, 343–349 (2004)

Mello CC and Conte D Jr, Revealing the world of RNA interference, Nature 431, 338–342 (2004)

Nykanen A et al., ATP requirements and small interfering RNA structure in the RNA interference pathway, Cell 107, 309–321 (2001)

Persengiev SP et al., Nonspecific, concentration-dependent stimulation and repression of mammalian gene expression by small interfering RNAs (siRNAs), RNA 10, 12–18 (2004)

Persson K and Ugozzoli LA, Guidelines for optimization of quantitative multiplex RT-PCR, BioRadiations 113, 16–23 (2004)

Schwarz DS et al., Asymmetry in the assembly of the RNAi enzyme complex, Cell 115, 199–208 (2003)

Ziauddin J and Sabatini DM, Microarrays of cells expressing defined cDNAs, Nature 411, 107–110 (2001)

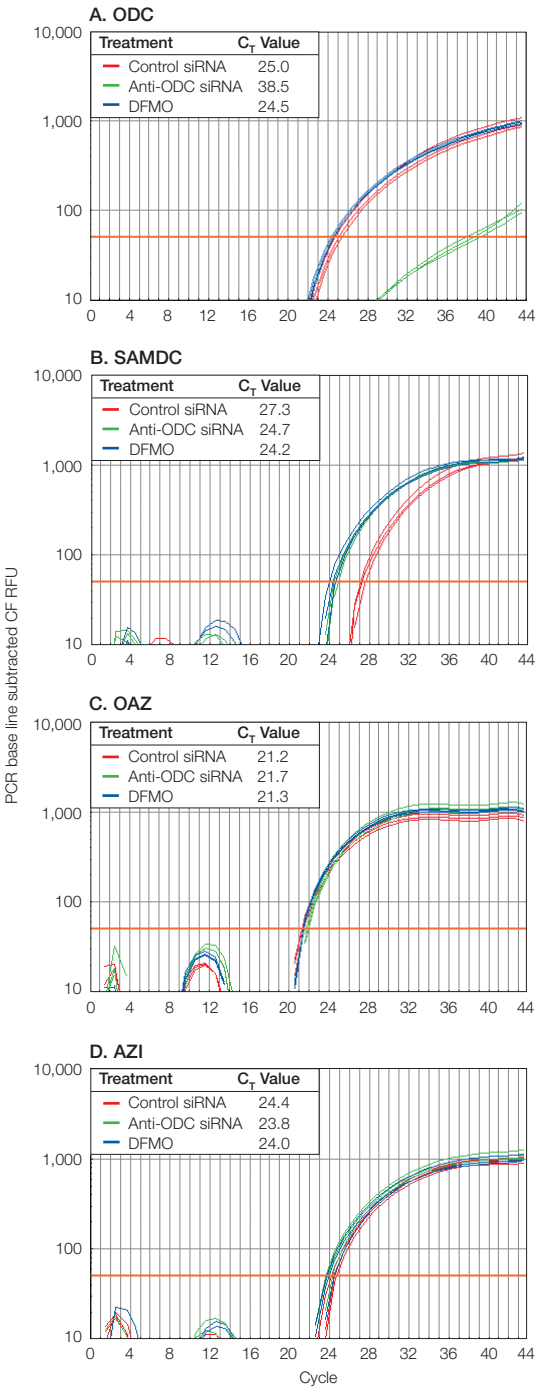

Fig. 6. Effects of siRNA transfection and DFMO treatment on gene expression in the polyamine biosynthetic pathway. Human primary fibroblasts were treated with either DFMO, anti-ODC siRNA, or a nonspecific control siRNA to investigate the effectiveness of siRNA-targeted degradation of ODC message vs. inhibition of the protein with DFMO. **A**, downregulation of ODC message levels by transfection of cells with siRNA targeted against the ODC gene. Note that treatment of the cells with DFMO produced no change in the ODC transcript levels. **B**, S-adenosylmethionine decarboxylase (SAMDC) transcript was highly upregulated by both DFMO and anti-ODC siRNA treatments. **C** and **D**, neither treatment affected message levels of the regulatory enzymes antizyme (OAZ) or antizyme inhibitor (AZI).

Optimization of TransFectin™ Lipid Reagent-Mediated Transfection for Different Cell Types

Angelika Bondzio, Nicole Walk, Jennifer Schön, and Ralf Einspanier
Institute of Veterinary Biochemistry, Free University of Berlin, Berlin, Germany

Introduction

The ability to introduce DNA into cells provides a powerful tool for studying the in vivo function and control of mammalian genes. Methods and reagents designed for nucleic acid delivery have received considerable attention, especially in protocols and discussions related to effective gene therapy strategies.

TransFectin lipid reagent is a mixture of a proprietary cationic lipid and colipid DOPE (1,2-dioleoylphosphatidylethanolamine). Cationic lipids, brought in contact with aqueous solutions under special conditions, form positively charged micelles or liposomes. These micelles associate with the negatively charged phosphates of nucleic acids and form spontaneous complexes with DNA or RNA. The lipid-DNA (or -RNA) complexes fuse or associate with the cell membrane via hydrophobic and electrostatic interactions, and the complex is then internalized (Zhou and Huang 1994, Remy et al. 1994).

It is important to optimize transfection conditions not only for each transfection method but also for every cell type. Cell density, duration of transfection, volume of medium during transfection, and ratio of lipid reagent to DNA are key factors for efficiency. In this article we describe the optimization of transfection with TransFectin monitored by a secreted alkaline phosphatase (SEAP) reporter gene assay. We compare two suspension cell types that are considered difficult to transfect: bovine peripheral blood mononuclear cells (PBMCs) and bovine B-lymphosarcoma BL3.1 cells (Anderson et al. 2004, Fenton et al. 1998). Additionally, we optimize the transfection efficiency for two adherent cell types: primary bovine oviductal cells and a calf pulmonary artery endothelial cell line (CPAE).

Methods

Cell Cultures

Lymphocytes were prepared from heparinized bovine peripheral blood after 1:1 dilution with PBS and Ficoll-Paque PLUS (Amersham Biosciences) density gradient centrifugation. Cells were cultured in RPMI-1640 medium (supplemented with 25 mM glucose, 10 mM HEPES, 1 mM sodium pyruvate,

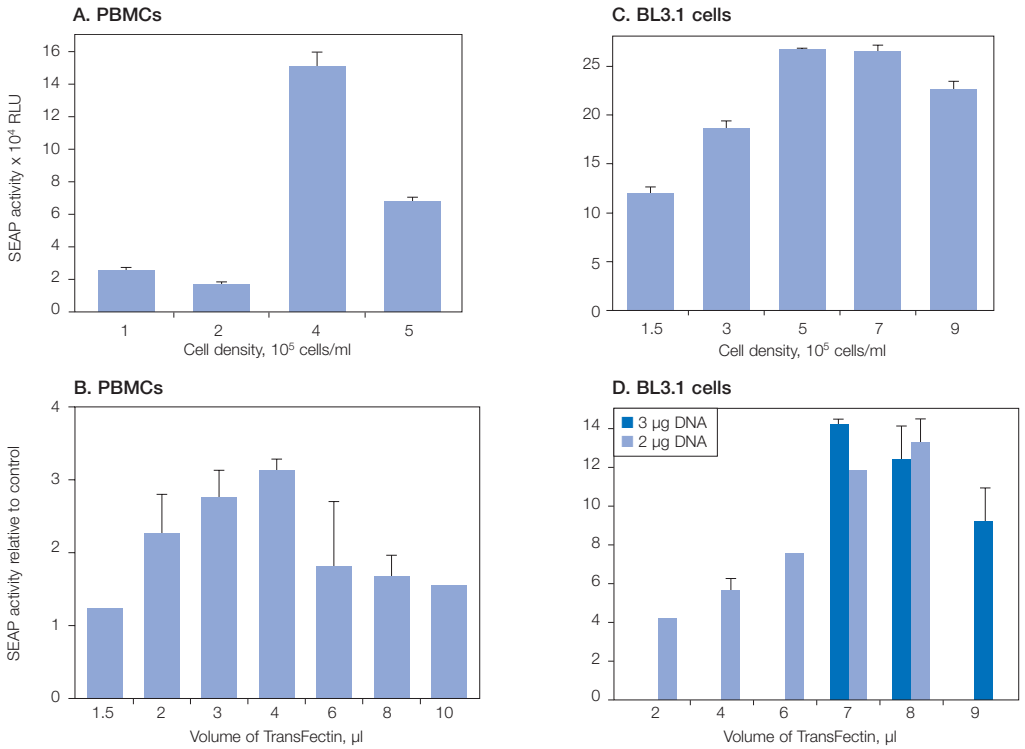

Fig. 1. Optimization of transfection conditions for suspension cells. Conditions were optimized for PBMCs (**A**, **B**) and BL3.1 cells (**C**, **D**). To evaluate the effect of cell density on transfection efficiency, cells were seeded at indicated concentrations 24 hr prior to transfection using 2 µg DNA (pTAL-SEAP2-control) and 4 µl (A) or 7 µl (C) TransFectin. To evaluate the effect of the amount of TransFectin on transfection efficiency, PMBCs (4 x 10^6/ml) were transfected using 2 µg DNA (pTAL-SEAP2-control) and indicated amounts of TransFectin (B). BL3.1 cells (5 x 10^5/ml) were transfected using 2 or 3 µg DNA (D). Cell culture supernatant was assayed 24 hr after transfection for SEAP activity. Values are expressed relative to those for transfection with a promoterless control plasmid (error bars indicate standard deviation; A, n = 4; B, n = 6; C, n = 4; D, n = 7).

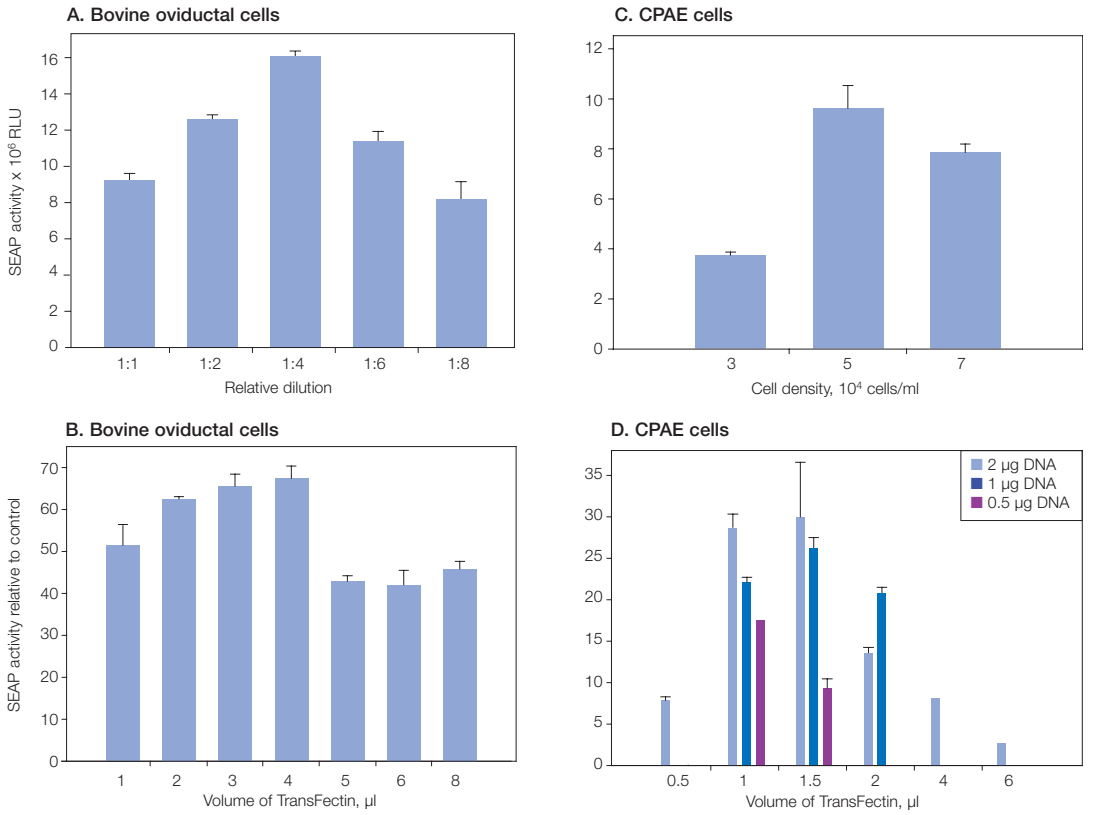

Fig. 2. Optimization of transfection conditions for adherent cells. Conditions were optimized for primary bovine oviductal cells (**A**, **B**) and CPAE cells (**C**, **D**). To evaluate the effect of cell density on transfection efficiency, primary bovine oviductal cells (A) were seeded at different dilutions of the initial cell suspension (a 1:4 dilution of the initial cell suspension prior to seeding corresponds to a cell density of 3–5 cells/ml in a 4 days' culture) and transfected using 2 µg DNA (pTAL-SEAP2-control) and 4 µl TransFectin. CPAE cells (C) were seeded at the indicated concentrations 24 hr prior to transfection using 2 µg DNA and 2 µl TransFectin. To evaluate the effect of the amount of TransFectin on transfection efficiency, primary bovine oviductal cells (3–5 x 10^4/ml) were transfected using 2 µg DNA (pTAL-SEAP2-control) and indicated amounts of TransFectin (B). CPAE cells (5 x 10^4/ml) were transfected using 0.5, 1, or 2 µg DNA (D). Cell culture supernatant was assayed 24 hr after transfection for SEAP activity. Values are expressed relative to those for transfection with a promoterless control plasmid (error bars indicate standard deviation; A, n = 4; B, n = 9; C, n = 4; D, n = 5).

and 10% FCS). The cell density was adjusted to 4 x 10^6 cells/ml. PBMCs were transfected after 20–24 hr of cultivation. The B-lymphosarcoma cell line, BL3.1, was obtained from ATCC (CRL-2306). Cell density of suspension cells BL3.1 was adjusted to 5 x 10^5/ml 1 day prior to transfection in RPMI-1640 medium.

Bovine oviductal cells were freshly prepared as described previously (Ulbrich et al. 2003) with some modifications: After centrifugation (550 x g for 5 min), 50 µl cell pellet was diluted in 20 ml Medium 199 (supplemented with 20 mM HEPES, 0.68 mM sodium pyruvate, 2.3 mM L-glutamine, and 10% FCS). This preparation was designated the initial dilution, and further dilutions were prepared for optimization of cell density. The cultivated primary cells were transfected 1 day after they became adherent (4 days after preparation). The CPAE cells (ATCC, CCL-209) were plated in a concentration of 5 x 10^4 cells/ml in MEM-Earle (supplemented with 0.1 mM nonessential amino acids, 1 mM sodium pyruvate, 2 mM glutamine, and 20% FCS) 1 day before transfection.

Each cell type was seeded on 24-well culture plates in 1 ml of the appropriate growth medium per ml and incubated at 37°C in a humidified 4.5% CO_2 atmosphere. The cell viability and proliferation were surveyed by colorimetric assay using WST-1 cell proliferation reagent (Roche) as recommended by the manufacturer.

Plasmids

Cells were transfected with the reporter plasmid TAL-SEAP2-control (Clontech), which contains the SEAP gene under control of the SV40 early promoter/enhancer or with a promoterless plasmid as negative control. In some cases cells were additionally transfected with a vector containing a β-galactosidase reporter gene under the control of the CMV promoter (CMVβ-Gal, kindly provided by Grant R MacGregor, Stanford University, USA).

Transfection Protocol for 24-Well Plate Format

For each well, DNA was diluted in 50 µl of serum-free growth medium and mixed gently briefly. TransFectin was prepared in 50 µl of serum-free growth medium per ml. Both solutions were combined, mixed gently, and incubated at room temperature for 20 min to allow TransFectin-DNA complex formation. The TransFectin-DNA mixture (100 µl) was added to the growth medium in each well and mixed gently by rocking the plate. Cells were incubated at 37°C and 4.5% CO_2.

Detection of Transfection Efficiency

The relative transfection efficiency was assessed by measuring SEAP activity in the culture media using a chemiluminescent SEAP reporter gene assay (Roche) according to the manufacturer's protocol. For quantitation, 25 µl of the transfected cell culture supernatant was used. The resulting light

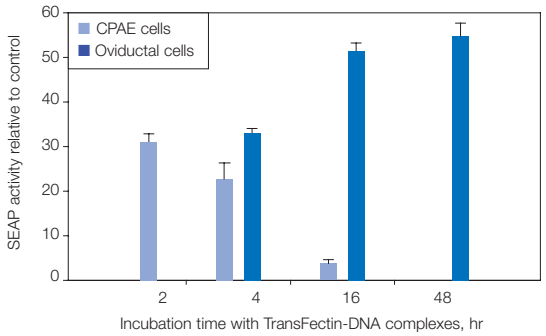

Fig. 3. Effect of incubation time on transfection efficiency of CPAE and bovine oviductal cells. CPAE cells (5 x 10^4/ml) were transfected with 1 µg DNA (pTAL-SEAP2-control) using 1.5 µl TransFectin, and bovine oviductal cells (3–5 x 10^4/ml) with 2 µg DNA and 4 µl TransFectin. Medium was replaced after indicated incubation times of cells with TransFectin-DNA complexes. Cell culture supernatant was assayed 24 hr (CPAE cells) or 48 hr after transfection (oviductal cells) for SEAP activity (error bars indicate standard deviation; n = 3).

signal was measured in a Sirius luminometer (Berthold). Values were expressed in relative light units (RLU) or as relative to the value from cells transfected with a promoterless plasmid. The β-galactosidase activity was estimated using a histochemical kit (Roche). Cells were stained with X-Gal 2 days after transfection.

Results

Suspension Cultures

Transfection conditions were optimized for lymphoid cells (PBMC and BL3.1). TransFectin/DNA ratio as well as cell density are known to affect transfection efficiency. Therefore, we examined in initial experiments the impact of cell density for each cell type, and then optimized the TransFectin/DNA ratio. With PBMCs, the highest SEAP activity was achieved by seeding 4 x 10^6 cells/ml 24 hr prior to transfection (Figure 1A). Figure 1B shows the results of TransFectin/DNA ratio optimization for PBMCs. The highest efficiency was achieved with 2 µg DNA and 4 µl TransFectin. Neither 1 µg nor 3 µg DNA resulted in higher efficiency on PBMCs at all tested TransFectin/DNA ratios (data not shown).

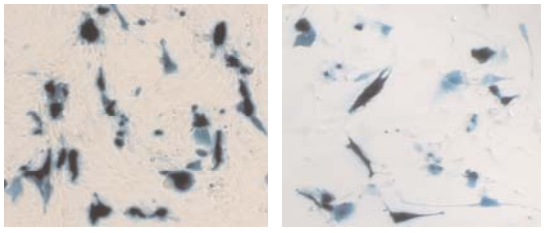

Fig. 4. Expression of β-galactosidase. Left, 3–5 x 10^4/ml bovine oviductal cells transfected with pCMVβ-Gal using 2 µg DNA and 4 µl TransFectin; **right**, CPAE cells transfected using 1 µg DNA and 1.5 µl TransFectin. β-Galactosidase activity was visualized 48 hr after transfection by histochemical staining.

Table 1. Recommended transfection conditions.

	PBMCs	BL3.1	Oviductal Cells	CPAE
Cell concentration	4 x 10^6/ml	5–7 x 10^5/ml	3–5 x 10^4/ml	5 x 10^4/ml
TransFectin/DNA ratio	4 µl/2 µg	7 µl/2 µg	4 µl/2 µg	1–1.5 µl/1–2 µg
Addition or replacement of medium after transfection	Add after 4 hr	Add after 12 hr	Not needed	Replace after 2 hr
Duration of transfection	24 hr	24 hr	48 hr	24 hr

Similar experiments were carried out with BL3.1 cells in suspension. For these cells, the best results were obtained with 5–7 x 10^5 cells/ml (Figure 1C). In comparison to the PBMCs, the established β-lymphosarcoma cell line, BL3.1, showed higher transfection efficiencies. The best results were achieved using 2–3 µg DNA and 7–8 µl TransFectin (Figure 1D).

Adherent Cells

Primary bovine oviductal cells revealed highest transfection efficiencies at a cell density of 3–5 x 10^4 adherent cells per ml (4 days' culture). This corresponded to a 1:4 dilution of the initial cell suspension prior to seeding (Figure 2A). As shown in Figure 2B, the best TransFectin/DNA ratio for this cell type was 4 µl/2 µg. Furthermore, CPAE cells can be transfected efficiently using a cell density of 5 x 10^4/ml (Figure 2C). Comparable results were obtained with 1–1.5 µl TransFectin and 1–2 µg DNA (Figure 2D). This cell line was very sensitive to TransFectin-DNA complexes. In contrast to primary bovine oviductal cells, the removal of the complexes 2 hr after transfection was essential for CPAE cells (Figure 3). Additionally, a vector containing a β-galactosidase reporter gene under the control of the CMV promoter was introduced and confirmed our previous results (Figure 4).

Conclusions

We evaluated transfection efficiency of bovine PBMCs, bovine B-lymphosarcoma cells, calf pulmonary aortic endothelial cells, and primary bovine oviductal cells using TransFectin lipid reagent. For the cell types tested, we recommend using a 24-well plate format under the transfection conditions detailed in Table 1. Remarkable transfection efficiencies were achieved by adjusting cell densities prior to transfection; quantities of TransFectin reagent and DNA; and incubation time of cells with TransFectin-DNA complexes. The results demonstrate the need for testing broad ranges of TransFectin/DNA ratios with each cell line in order to achieve maximum transfection efficiencies. TransFectin turned out to be highly efficient in these cell types, which are considered difficult to transfect.

References

Anderson MD et al., Transformation studies with a human T-cell leukemia virus type 1 molecular clone, J Virol Methods 116, 195–202 (2004)

Fenton M et al., The efficient and rapid import of a peptide into primary B and T lymphocytes and a lymphoblastoid cell line, J Immunol Methods 212, 41–48 (1998)

Remy JS et al., Gene transfer with a series of lipophilic DNA-binding molecules, Bioconjug Chem 5, 647–654 (1994)

Ulbrich SE et al., Expression and localization of estrogen receptor alpha, estrogen receptor beta and progesterone receptor in the bovine oviduct in vivo and in vitro, J Steroid Biochem Mol Biol 84, 279–289 (2003)

Zhou X and Huang L, DNA transfection mediated by cationic liposomes containing lipopolylysine: characterization and mechanism of action, Biochim Biophys Acta 1189, 195–203 (1994)

Real-Time PCR Assay Optimization for Allelic Discrimination of a Glu298Asp Polymorphism in the Constitutive Endothelial Nitric Oxide Synthase Gene

Cristina Tonello,[1]* Renata Bracale,[1] and Tommaso Mancuso[2] [1]Department of Preclinical Sciences, Luigi Sacco Hospital, Via G.B. Grassi 74, 20157, Milano, Italy and [2]Bio-Rad Laboratories S.r.l., Via Cellini 18/A, 20090 Segrate (Milano), Italy *Corresponding author

Introduction

Nitric oxide (NO) is synthesized from L-arginine by a family of NO synthase (NOS) isoforms. Constitutively expressed NOS isoforms, endothelial NOS (eNOS) and neuronal NOS (nNOS), are likely the major contributors to whole-body NO production. Many studies have strongly associated polymorphisms of the *eNOS* gene with increased risk of hypertension, cardiovascular disease, coronary spastic angina, myocardial infarction, and stroke, but the results are not always conclusive (Wang and Wang 2000). In particular, Yoshimura et al. (1998) identified a Glu298Asp variant in exon 7 of the *eNOS* gene that was more frequent in patients with coronary spasm, but in studies of an elderly population in Australia, Liyou et al. (1998) could find no association of this variant with coronary artery disease. Recently, various *eNOS* polymorphisms have been reported to be associated with type 2 diabetes and the insulin resistance syndrome (Monti et al. 2003). Moreover, NO impairment has been hypothesized as an early step in the development of metabolic syndrome (Nisoli et al. 2003). Metabolic syndrome is a collection of cardiovascular risk factors, including insulin resistance, abdominal obesity, hypertension, and hypertriglyceridemia, that increase the chance of developing heart disease, stroke, and diabetes. The question of whether subpopulations of humans suffering from metabolic syndrome have defects in *eNOS* gene expression awaits an answer from genetic analysis. Our aim was to investigate the relation between the Glu298Asp polymorphism in *eNOS* exon 7 and metabolic syndrome. For this purpose, we set up a fast and reliable real-time PCR allelic discrimination method.

Methods

Most assays for mutation detection combine amplification of the DNA sequence that spans the target polymorphic nucleotide with allele-specific oligonucleotide (ASO) probes (Wallace et al. 1979). Real-time PCR assays can be devised to combine DNA amplification with probing of specific sequences, allowing amplification and detection in a homogeneous, all-in-one-tube system with reliable genotype assignment. Real-time PCR also minimizes the time needed for experiments, since 48 patient samples can be analyzed simultaneously in duplicate. To validate such a real-time PCR genotyping system, a comparison should be made to established methods. For this comparison, we analyzed samples from 20 patients and 20 control subjects by means of both a classical PCR-RFLP method and real-time PCR allelic discrimination.

Genomic DNA (gDNA) was purified from peripheral blood leukocytes as previously reported (Miller et al. 1988). For PCR-RFLP, a specific *eNOS* genomic fragment covering the Glu298Asp polymorphism was amplified in the iCycler iQ® system followed by endonuclease digestion. Primer pairs were as follows: sense 5'-TCCCTGAGGAG-GGCATGAGGCT-3'; and antisense 5'-TGAGGG-TCACACAGGTTCCT-3'. The amplification mix (25 µl) consisted of 12.5 µl 2x iQ™ supermix, 500 ng gDNA, and 300 nM of each primer. After initial denaturation and hot-start DNA polymerase activation (3 min at 95°C), amplification was performed for 30 cycles (1 min at 94°C, 1 min at 61°C, and 1 min at 72°C). The resulting 457 bp products were incubated at 37°C for at least 20 hr with 8 U of the restriction enzyme *Ban*II. In case of polymorphism at position 1917 of the *eNOS* gene, typically a G to T substitution, the *Ban*II restriction site is lost.

For real-time PCR experiments, primers and ASO hydrolysis probes were designed by Beacon Designer 2.1 software (PREMIER Biosoft International) and purchased from Qiagen GmbH (Hilden, Germany); they are shown in Table 1. Forward and reverse primers were used in a PCR fluorescent detection system with the intercalating dye SYBR Green I to check for product specificity. Each sample (25 µl) contained 12.5 µl iQ™ SYBR® Green supermix, 0.1 µM of each primer, and scalar quantities of gDNA (200, 100, 50, and 25 ng). PCR cycles were programmed on an iCycler iQ real-time PCR detection system and consisted of hot-start incubation (3 min at 95°C) and amplification for 40 cycles (10 sec at 95°C and 10 sec at 62°C). Generation of a melt curve starting at 55°C with increments of 0.5°C every 10 sec followed the amplification program.

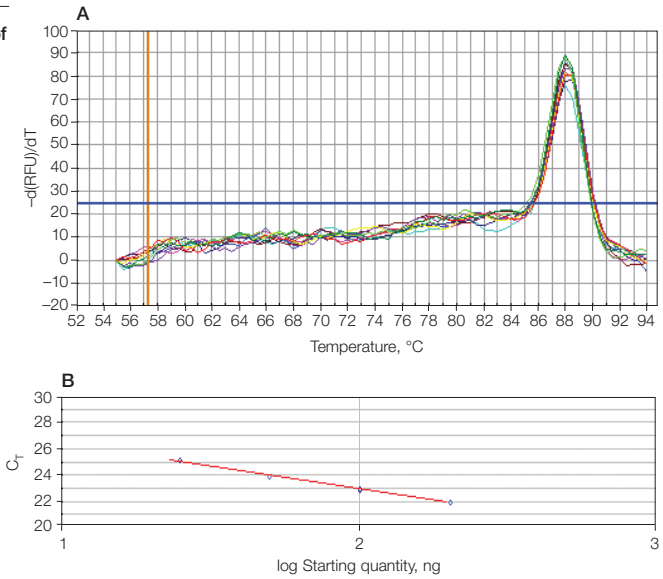

Fig. 1. Specificity of PCR amplification. **A**, melt curve; **B**, standard curve. Results using a reaction mix with SYBR Green I and the primers shown in Table 1. Standard curve had slope = –3.492, intercept = 29.39, r^2 = 0.997.

In order to find the specific discriminating conditions for the ASO probes, the iCycler iQ gradient feature was used to optimize annealing temperature (Ugozzoli 2003). Duplicate PCR reactions were carried out in 25 µl containing 12.5 µl iQ supermix, 0.1 µM of each primer, 0.075 mM of each ASO probe, and 50 ng human gDNA. PCR conditions were the same as for the SYBR Green I test, except for annealing/extension temperature. This was performed at 58.0, 59.0, 60.5, 61.0, 61.5, 62.0, 62.5, and 63.0°C (temperature gradient). All subsequent analyses for test validation were performed with the same conditions except for the annealing/extension temperature, fixed at 62.0°C.

Table 1. Sequence of primers and ASO probes for Glu298Asp *eNOS* polymorphism analysis. The polymorphic site is underlined. Abbreviations: WT, wild type; BHQ, Black Hole Quencher.

Name	Sequence
eNOS-Rev primer	5'-GGGGGCAGAAGGAAGAGT-3'
eNOS-Fwd primer	5'-CCAGGAAACGGTCGCTTC-3'
eNOS-WT probe	5'-[Texas Red]-CTGGGGGCTCATCT-GGG-[BHQ2]-3'
eNOS-Mutant probe	5'-[6-FAM]-CTGGGGGATCATCTGGG-[BHQ1]-3'

Results

PCR Specificity

To check the specificity of PCR amplification using the primers shown in Table 1, we amplified some samples in the presence of SYBR Green I. The iCycler iQ system was programmed to perform a two-step (denaturation and annealing/extension) PCR protocol, and melt-curve analysis followed amplification. Figure 1A clearly shows a single sharp peak, indicating amplification of a single product and the absence of nonspecific fragments and primer-dimers at an annealing temperature of 62°C. In addition, high PCR efficiency and a good dynamic range were observed (Figure 1B). Primer-dimers and nonspecific PCR fragments were also not observed within the temperature range used subsequently (59–64°C; data not shown).

Assay for Allelic Discrimination

The differentially labeled wild-type (WT) and mutant ASO probes were mixed in the same reaction with the PCR primers and subjected to an annealing temperature gradient from 59 to 64°C. Some results from the optimization experiment are shown in Figure 2. For both the WT and mutant probes, reactions worked well within the range 62–64°C. Results obtained using annealing temperatures lower than 62°C showed lack of specificity, especially for the WT ASO probe. For example, the amplification plot generated at 60°C (Figure 2A) shows that the WT probe labeled with Texas Red hybridized to the WT PCR product (red trace), but also cross-hybridized to the homozygous mutant PCR product (blue trace).

Validity

After assay optimization, 20 metabolic syndrome patients and 20 healthy control subjects were genotyped using the real-time PCR method described. The results (Figure 3) were compared to those obtained by PCR-RFLP analysis (Figure 4). The genotyping results were the same for all 40 samples analyzed (100% accordance), confirming the validity of the method. Table 2 summarizes the results for both methods.

Table 2. Number and percentage of metabolic syndrome patients and control subjects showing the different *eNOS* variants.

Genotype	Metabolic Syndrome Patients		Control Subjects	
WT (GG)	8	(40%)	10	(50%)
Heterozygote (GT)	9	(45%)	8	(40%)
Mutant (TT)	3	(15%)	2	(10%)
Total	20	(100%)	20	(100%)

Conclusions

We have shown a robust assay for allelic discrimination of the Glu298Asp polymorphism in the *eNOS* gene. This assay shows the accuracy, specificity, reliability, and processivity of a real-time PCR genotyping system. Typically, 48 samples can be processed in 1.5 hr in duplicate, so hundreds of patients can be genotyped in a few days. The data reported in Table 2 show a very slight prevalence of *eNOS* mutants and heterozygotes in metabolic syndrome patients compared with control subjects. In any case, the number of subjects tested in this preliminary study is too few to draw any conclusions. Our group has so far recruited more than 400 metabolic syndrome patients and 200 healthy control subjects. These will be part of a wider study that we hope will shed light on the possible involvement of *eNOS* defects in the genesis of metabolic syndrome.

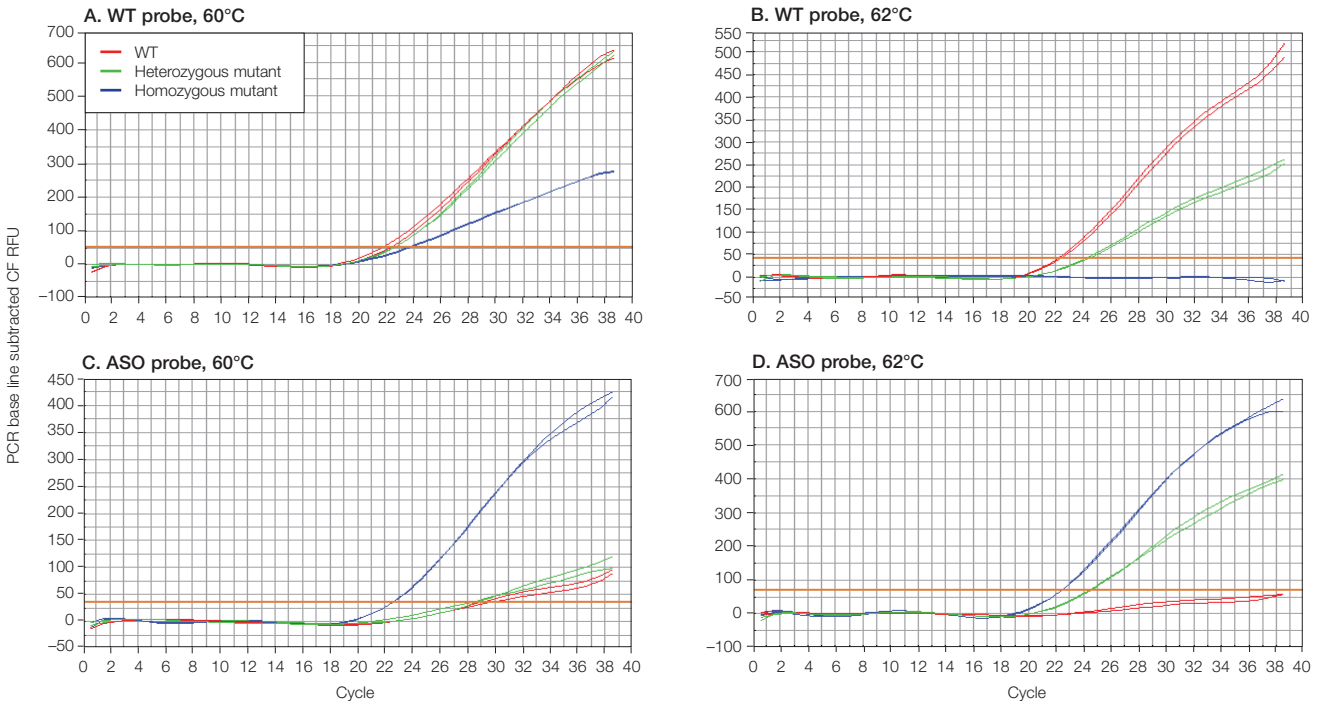

Fig. 2. Amplification plots for WT (A and B) and mutant (C and D) ASO probes. PCR was carried out with an annealing/extension step at 60°C (**A** and **C**) or at 62°C (**B** and **D**). The traces for each genotype were clearly distinguishable at 62°C.

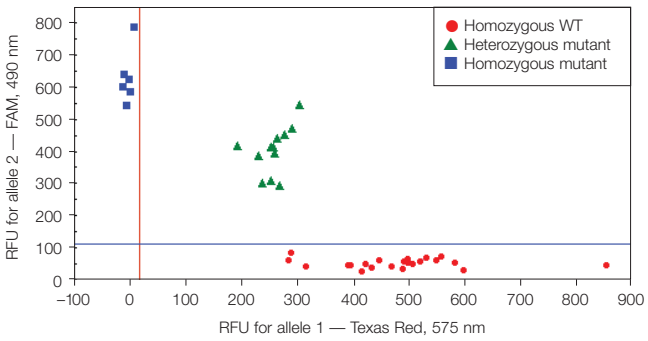

Fig. 3. Example of an allelic discrimination graph for the Glu298Asp polymorphism in the *eNOS* gene. Twenty samples were analyzed in duplicate in a single analysis.

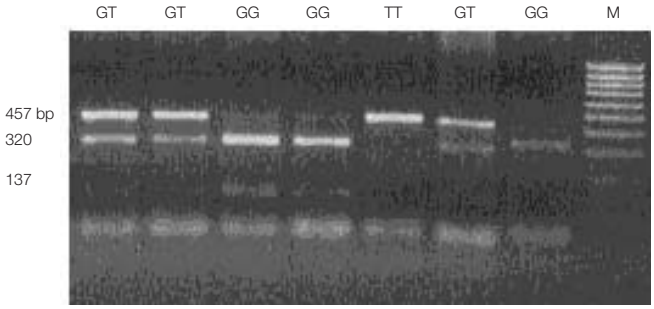

Fig. 4. Example of a classical PCR-RFLP analysis for Glu298Asp polymorphism in the *eNOS* gene. Samples from seven individuals were run on a 2% agarose gel, stained with ethidium bromide, and photographed under UV transillumination. GG = WT homozygote; GT = heterozygote; TT = mutant homozygote; M, DNA size markers.

References

Liyou N et al., Coronary artery disease is not associated with the E298→D variant of the constitutive, endothelial nitric oxide synthase gene, Clin Genet 54, 528–529 (1998)

Miller SA et al., A simple salting out procedure for extracting DNA from human nucleated cells, Nucleic Acids Res 16, 1215 (1988)

Monti LD et al., Endothelial nitric oxide synthase polymorphisms are associated with type 2 diabetes and the insulin resistance syndrome, Diabetes 52, 1270–1275 (2003)

Nisoli E et al., Mitochondrial biogenesis in mammals: the role of endogenous nitric oxide, Science 299, 896–899 (2003)

Ugozzoli LA, The gradient feature: use in optimization of allelic discrimination assays, Bio-Rad bulletin 3024 (2003)

Wallace RB et al., Hybridization of synthetic oligodeoxyribonucleotides to phi chi 174 DNA: the effect of single base pair mismatch, Nucleic Acids Res 6, 3543–3557 (1979)

Wang XL and Wang J, Endothelial nitric oxide synthase gene sequence variations and vascular disease, Mol Genet Metab 70, 241–251 (2000)

Yoshimura M et al., A missense Glu298Asp variant in the endothelial nitric oxide synthase gene is associated with coronary spasm in the Japanese, Hum Genet 103, 65–69 (1998)

2-D Gel Electrophoresis Troubleshooting

Bio-Rad has been in the business of electrophoresis for over 15 years, and during that time, has answered many questions related to 2-D gel analysis. Questions often arise regarding how to perform and optimize elements of this separation technique. This article addresses three common questions.

How to Estimate the Isoelectric Point (pI) of a Protein

The pI of a protein is typically determined from its focused position on an immobilized pH gradient (IPG) strip. IPG strips are created by grafting a pH gradient directly to a polyacrylamide matrix. The pH gradient in these strips is fixed in the gel, is reproducible in commercially produced strips, and remains unchanged during isoelectric focusing (IEF). Two types of IPG strips are available, linear and nonlinear, and both can be used for pI estimation.

When linear IPG strips are used, it is acceptable to assume that the pH gradient extends linearly between the given pH extremes. The pI of individual proteins separated on these strips can then be derived using the linear relationship between the pH range and the length of the strip. For example, a protein that focuses at the middle of a linear pH 4–7 IPG strip will have an estimated pI of 5.5 (Figure 1A). When nonlinear IPG strips are used, the pH profile of the IPG strip must be obtained from the manufacturer (Figure 1B); without the exact pH profile of the strip, the pI estimate will be less accurate. The same strategy that is used with IPG strips can be applied for protein spots on 2-D gels, though with less accuracy due to swelling or shrinking of the gels. Note also that the chemical environment of a protein can influence its apparent pI; therefore, the estimated pI may differ under various experimental conditions.

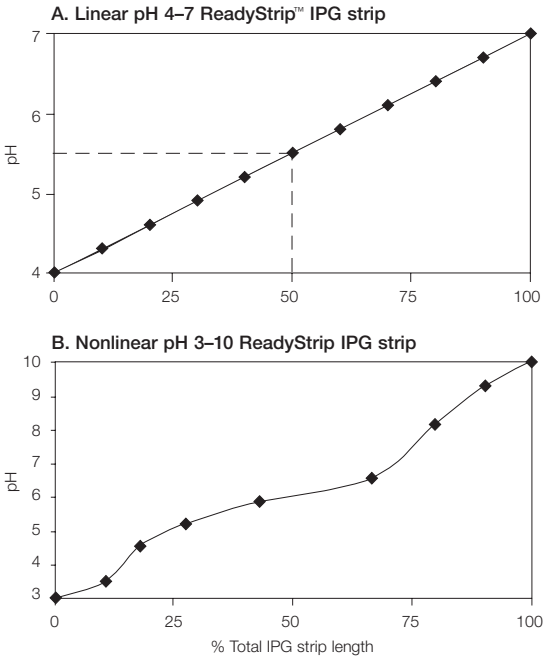

Fig. 1. Estimating the pI of a protein from its position along an IPG strip. By plotting the pH of an IPG strip as a function of its length, the pI of a protein may be derived from its focused position on that strip. **A**, the pH vs. length relationship of a linear pH 4–7 IPG strip, indicating how to estimate the pI of a protein that migrates to 50% of the gel length; **B**, the pH vs. length relationship of a nonlinear pH 3–10 IPG strip.

How to Determine Optimal Focusing Conditions

Focusing conditions vary with sample complexity, protein load, pH range, and strip length. IEF based on IPG technology has been used for years in proteomics research, and Bio-Rad, as a major supplier in the field, provides proven protocols for a number of wide, medium, and micro-range IPG strips.

As a rule of thumb, the narrower the pH gradient, the longer the IPG strip, and the higher the protein load, the more total volt-hours are required to achieve steady-state separations, which are the prerequisite for good reproducibility from run to run. Table 1 provides recommendations for focusing conditions at different pH ranges and strip lengths. Underfocusing of the protein sample will lead to horizontal streaking in the final 2-D map, but severe overfocusing should be avoided as well. If severe horizontal streaking occurs when following the recommendations of Table 1, it may be necessary to determine optimum focusing conditions empirically. This can be accomplished by programming the PROTEAN® IEF cell for a total volt-hour value that is the maximum recommended for the particular IPG strip in Table 1. Then, focus three strips using this program. As the PROTEAN IEF cell reaches the lower volt-hour value to be tested, pause the instrument and remove a strip. Before resuming the focusing run, be sure to edit the program to account for the number of strips remaining. As each strip is removed, equilibrate the proteins and run the SDS-PAGE step. Comparison of the three sets of resulting 2-D gels will help identify the appropriate focusing conditions.

Keep in mind that contaminants in the protein sample, protein overloading, and separation in the basic-pI range may contribute to horizontal streaking as well. Contaminants can be easily removed by the ReadyPrep™ 2-D cleanup kit (catalog #163-2130). Prevention of protein overloading can be addressed by recommendations provided in Table 2, which illustrates how much protein should be loaded based on the length of the strip and type of stain used for visualization. Finally, to ensure success for micro-range and basic-range IPG strips, follow two additional steps. The first step is to treat the sample using the ReadyPrep reduction-alkylation kit

(163-2090). This reduces streaking caused by disulfide bond formation. Disulfide bond formation is more problematic with micro-range and basic-range proteins. The second additional step is to use cup loading when loading samples for IEF.

How to Improve Coverage of High Molecular Weight (HMW) Proteins on 2-D Maps

A substantial portion of HMW proteins (>150 kD) are rather hydrophobic and are therefore difficult to solubilize in standard urea-containing lysis and rehydration solutions. The addition of stronger denaturing agents and detergents, such as thiourea and ASB-14, to the lysis and rehydration solution may be helpful to better dissolve these proteins. Nevertheless, even solubilized HMW proteins may not always enter the IEF gel matrix or may be poorly transferred from the first- to the second-dimension gel. Sample addition using the cup loading technique rather than the more commonly used in-gel rehydration strategy may improve entry of HMW proteins into the IPG gel matrix. Hydrophobic interactions between the proteins and the wall of the tray, and size exclusion effects of the gel matrix are possible reasons for poor transfer of HMW proteins by in-gel rehydration. However, if samples must be applied by in-gel rehydration, applying low voltages (30–50 V) for active strip rewelling is often much more effective than passive loading.

Reducing sample complexity through fractionation may also enhance the representation of HMW proteins on 2-D gels. The application of samples that have been fractionated by liquid-phase IEF using the Rotofor® cell instead of crude samples may also improve the qualitative and quantitative display of HMW proteins on 2-D gels. A combination of size exclusion chromatography or SDS-PAGE with either 1-D gels or the Model 491 prep cell may also be an appropriate strategy to enrich for HMW proteins.

For other 2-D questions, several troubleshooting resources are available from Bio-Rad. Many frequently asked questions are answered in our searchable database of frequently asked questions (FAQs), available online at **consult.bio-rad.com**. Alternatively, visit our newest resource, the 2-D Doctor, at **www.expressionproteomics.com** (see page 2).

Table 1. Focusing conditions for ReadyStrip IPG strips of various lengths at various pH ranges.

pH Range		Strip Length	Start Voltage	End Voltage	Set Time	Volt-Hours	Ramp Speed	Temperature
pH 3–10, 3–10 NL, 4–7, 5–8		7 cm	0 V	4,000 V	—	8,000–10,000	Rapid	20°C
		11 cm	0 V	8,000 V	—	20,000–35,000	Rapid	20°C
		17 cm, 18 cm	0 V	10,000 V	—	40,000–60,000	Rapid	20°C
		24 cm	0 V	10,000 V	—	60,000–80,000	Rapid	20°C
pH 3–6		7 cm	0 V	4,000 V	—	8,000–10,000	Rapid	20°C
		11 cm	0 V	8,000 V	—	15,000–20,000	Rapid	20°C
		17 cm, 18 cm	0 V	10,000 V	—	30,000–40,000	Rapid	20°C
		24 cm	0 V	10,000 V	—	40,000–55,000	Rapid	20°C
pH 7–10		7 cm	0 V	4,000 V	—	8,000–15,000	Rapid	20°C
		11 cm	0 V	8,000 V	—	20,000–30,000	Rapid	20°C
		17 cm, 18 cm	0 V	10,000 V	—	40,000–50,000	Rapid	20°C
		24 cm	0 V	10,000 V	—	60,000–70,000	Rapid	20°C
pH 3.9–5.1, 4.7–5.9	Step 1	All lengths	0 V	250 V	15 min	—	Rapid	20°C
	Step 2	7 cm	250 V	4,000 V	1 hr	—	Slow	20°C
		11 cm	250 V	8,000 V	1 hr	—	Slow	20°C
		17 cm, 18 cm	250 V	10,000 V	2 hr	—	Slow	20°C
		24 cm	250 V	10,000 V	2 hr	—	Slow	20°C
	Step 3	7 cm	4,000 V	4,000 V	—	10,000–20,000	Rapid	20°C
		11 cm	8,000 V	8,000 V	—	20,000–30,000	Rapid	20°C
		17 cm, 18 cm	10,000 V	10,000 V	—	30,000–45,000	Rapid	20°C
		24 cm	10,000 V	10,000 V	—	60,000–90,000	Rapid	20°C
pH 5.5–6.7, 6.3–8.3 (Steps 1 and 2 as above)	Step 3	7 cm	4,000 V	4,000 V	—	20,000–30,000	Rapid	20°C
		11 cm	8,000 V	8,000 V	—	30,000–45,000	Rapid	20°C
		17 cm, 18 cm	10,000 V	10,000 V	—	45,000–60,000	Rapid	20°C
		24 cm	10,000 V	10,000 V	—	60,000–90,000	Rapid	20°C

Table 2. Recommended IPG strip loading conditions. Volumes shown apply to rehydration/sample buffer used for loading protein sample onto IPG strip.

	IPG Strip Length				
	7 cm	**11 cm**	**17 cm**	**18 cm**	**24 cm**
Rehydration volume per strip	125 µl	185 µl	300 µl	315 µl	410 µl
Protein load					
Silver stain*	5–20 µg	20–50 µg	50–80 µg	50–80 µg	80–150 µg
Coomassie Blue G-250 stain	50–100 µg	100–200 µg	200–400 µg	200–400 µg	400–800 µg

* Applicable to SYPRO Ruby protein gel stain as well.

Improving Reliability and Reproducibility of Real-Time PCR Reactions Sealed With Clear Films

Introduction

Clear adhesive sealers are a convenient sealing option for real-time quantitative PCR because they transmit light effectively and are easy to use. When choosing a sealer, however, it is important to consider its sealing strength as well as its clarity. Many adhesive sealers lack the aggressive adhesion necessary for properly sealing a PCR plate, and therefore can produce inconsistent results.

Improper sealing of reaction wells during thermal cycling is problematic because it can allow the aqueous portion of the sample to evaporate, increasing the concentration of the remaining reagents. This can lead to variability in PCR success, efficiency, and accuracy. Some reactions may fail completely, showing no product, while others may have a nonexponential increase in fluorescence, a late cycle threshold (C_T), or an abnormal melt profile. Such variability complicates the interpretation of results, since it may not be obvious which data are inaccurate.

Many plate sealers marketed for PCR are promoted as being superior due to an appearance of high clarity, without reference to sealing efficiency. The implication is that sealers that appear clearer or thinner would allow greater light transmission and perhaps greater sensitivity or earlier C_T values. But the potential for small improvements in sensitivity must be weighed against the potential loss in accuracy if inadequate sealing leads to questionable results.

We measured reaction variability of Microseal® 'B' seals (catalog #MSB-1001) and two other clear sealers that are marketed for real-time PCR to determine which sealers produced the most desirable results. All seals were tested with and without an optical compression pad (ADR-3296). The Microseal 'B' seals and compression pad are also available in an optical film sealing kit (MSO-1001). Reactions sealed with optical cap strips (TCS-0803) were run for comparison. We also compared the light transmission of all sealers. The results support the view that tight sealing is a more important consideration than apparent clarity for obtaining consistent results in real-time PCR.

Analysis of Reaction Variability

To assess reaction variability, human DNA was used as template in SYBR Green I quantitative PCR reactions. Initial template amount was 10^3 copies; final concentration was 2.0 ng/µl. Twenty-four 20 µl samples were arranged in a checkerboard pattern distributed across six columns and eight rows of a Hard-Shell® 96-well PCR plate with white wells and white shells (HSP-9655). Samples were amplified using a Chromo4™ real-time PCR detection system. All tests were run in triplicate.

Fluorescence traces and melt profiles were examined to assess reaction variability and determine sealing failure rate. Sealing failures were quantified in three steps: First, wells with a cycle threshold (C_T) or melting temperature (T_m) clearly different from the majority of wells were eliminated and counted as failures. Next, the mean C_T and T_m for the remaining wells were calculated. Finally, any wells in which the C_T or T_m differed by more than ±0.75 cycles from the mean were counted as failures. The standard deviation (SD) of the C_T of successful reactions was used as a measure of reaction variability.

When film seals were used without the compression pad, all test samples exhibited some level of sealing failure and greater reaction variability compared to caps (Figure 1; Table 1). Microseal 'B' seals had considerably fewer reaction failures (8/72 reactions in three runs) than film of either competitor A (29/72 reactions) or competitor B (27/72 reactions). Microseal 'B' seals also showed less reaction variability than for competitors A and B (Table 1). In contrast, no sealing failures occurred and reaction variability was considerably lower when optical cap strips were used.

Use of the compression pad further reduced reaction variability and virtually eliminated sealing failures. When the compression pad was used, no more than 1 of 72 reactions failed for any sealer. Reaction variability was improved for all film seals, but all reactions continued to exhibit greater variability than with optical caps (Table 1).

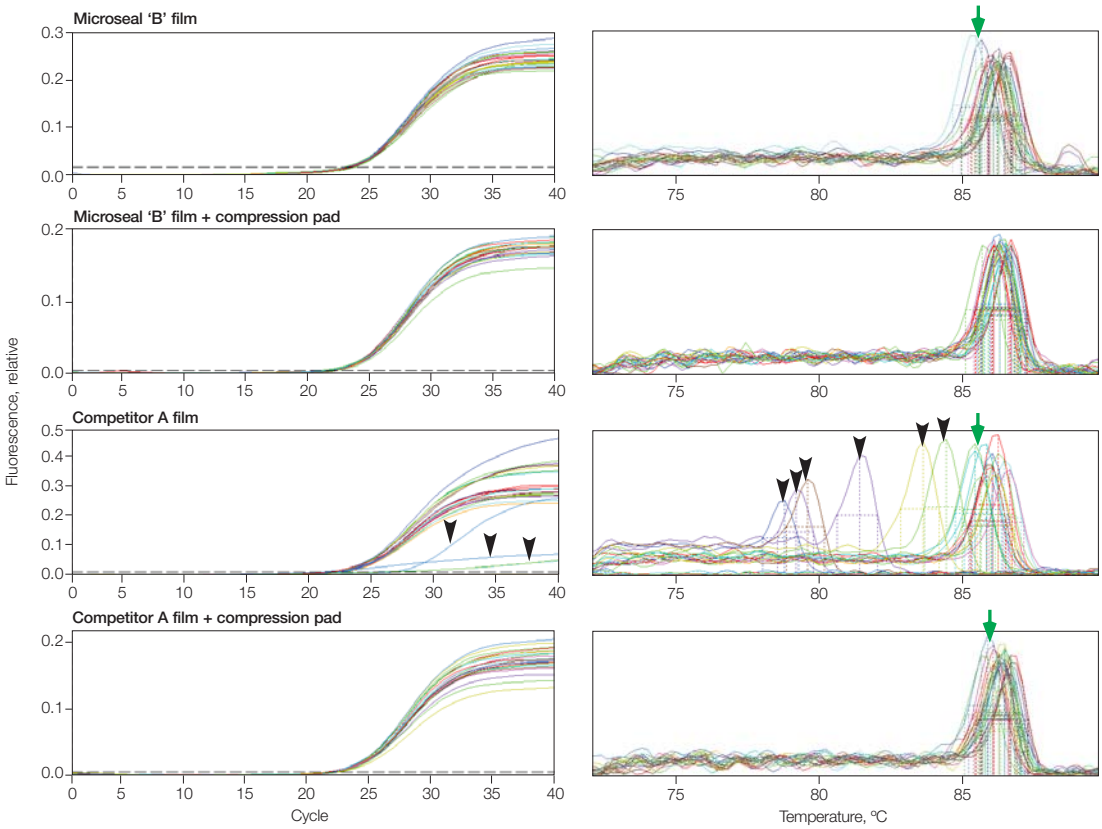

Fig. 1. Comparison of real-time PCR results with various plate film sealers. Left panels, amplification profiles. With the competitor's seals, there were reaction failures (arrowheads) when the pad was not used. **Right panels**, melting profiles. With the competitor's seals, there were spurious melt peaks (arrowheads) when the pad was not used. In addition, increased variability in the melting temperature (green arrows) was consistently observed with the competitor's seals (both with and without pads), but not with Microseal 'B' film plus a pad. Data shown are the best of three runs performed with each test condition.

Analysis of Light Transmission

To measure light transmission, fluorescence was measured for each sealer in each of the four channels of the Chromo4 real-time system. Different experimental plates, containing different channel-specific reporter dyes (FAM, HEX, ROX, and Cy5) attached to a 15-base poly(T) oligonucleotide, were prepared for each channel. Reaction components were assembled and 20 µl volumes were pipetted into each well of Hard-Shell 96-well PCR plates with white wells and white shells.

Each plate was read 5 times at 25°C, first without a sealer and then with each of the sealers. After each series of reads, the sealer was removed and another sealer was placed on the plate. For each sealer, raw fluorescence measurements (without background subtraction) from five reads of all 96 wells were averaged for each channel, and well-to-well variability was calculated. Light transmission for each sealer was then calculated by dividing the raw signal obtained with the sealer by the raw signal obtained with no sealer, and was expressed as a percentage.

Despite obvious differences in thickness, apparent clarity, or both among the film seals, light transmission at the four wavelengths measured was very similar. The fluorescent signals measured for the three seals fell within 10% of each other, and no sealer exhibited problematic signals. When the compression pad was added, transmission was reduced about 30% — to a level similar to transmission through optical caps (Figure 2).

Summary and Recommendations

The results of this study demonstrate that effective sealing is important for achieving low variability and a high success rate in quantitative PCR. Although some suppliers emphasize the clear appearance of their optical sealing films, we found no significant difference in light transmission among the different sealers, indicating that such differences are not

Table 1. Reaction successes and failures for three film seals with or without a compression pad.

Sealer	Success Rate (% of Wells)	C_T Spread (SD of Successful Reactions)	Total # of Failed Wells	# Failed With Low T_m	# Failed With Early C_T	# Failed With Late C_T
Microseal 'B' seal	89	0.48	8	6	0	6
Microseal 'B' seal + pad	99	0.39	1	0	0	1
Competitor A	60	0.67	29	29	8	6
Competitor A + pad	100	0.57	0	0	0	0
Competitor B	63	0.77	27	18	2	19
Competitor B + pad	99	0.51	1	0	1	0
Optical cap strips	100	0.25	0	0	0	0

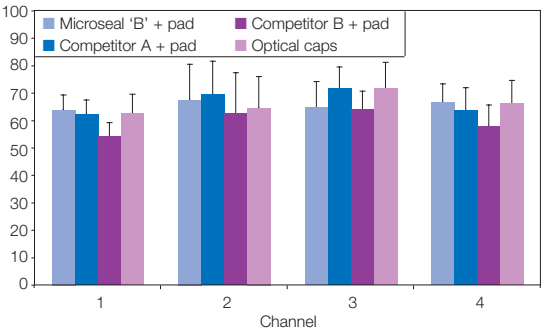

Fig. 2. Effect of using a compression pad. Results using three commercially available films to seal a plate were compared to those with optical caps. Values shown are average ± SD of the percentage of the signal obtained from the four channels of the Chromo4 system with unsealed plates.

responsible for differences in success rate. The sealing methods that produced the lowest variability were optical caps, followed by sealing films with a compression pad.

Our major findings were, first, that Microseal 'B' seals provide the most consistent sealing of the three adhesive seals tested. Second, addition of a compression pad to uniformly distribute the pressure of the heated lid across the sample holder greatly improved the sealing of all films but reduced light transmission slightly, to a level comparable to that of optical caps. Finally, the variability of reactions sealed with adhesive seals was greater than that achieved with optical caps, even when the compression pad was used.

These findings indicate that the choice of sealer should be dictated by the specific needs of an experiment. If obtaining uniform results from all wells is essential, optical caps are preferable to any adhesive seal. On the other hand, if the need for high sensitivity outweighs the need for optimal consistency, use of Microseal 'B' seals without a compression pad may be desirable. When ease of sealing is a greater concern than optimal uniformity, we recommend using Microseal 'B' seals with a compression pad. Although the compression pad slightly reduced light transmission, this effect did not significantly alter the C_T values obtained.

Ordering Information

Catalog #	Description
MSO-1001	Optical Film Sealing Kit, for 96-well plates, includes optical compression pad, 100 Microseal 'B' clear adhesive seals
MSB-1001	Microseal 'B' Clear Adhesive Seals, 100
ADR-3296	Optical Compression Pad, for improved film sealing of 96-well plates in real-time systems
TCS-0803	Optical Flat 8-Cap Strips, for 0.2 ml tubes and plates, ultraclear, 120
HSP-9655	Hard-Shell 96-Well PCR Plates, white well, white shell, rigid two-component design, 50

NEW LITERATURE

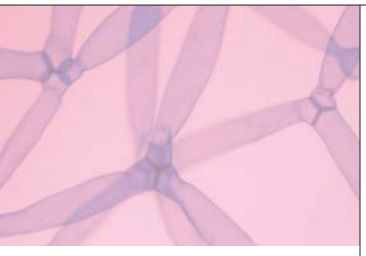

Amplification

- Chromo4™ four-color real-time PCR system brochure (bulletin 5215)
- DNA Engine Opticon® real-time PCR systems brochure (bulletin 5216)
- DNA Engine® line thermal cycler brochure (bulletin 5217)
- DNA Engine Tetrad® 2 Peltier thermal cycler flier (bulletin 5219)
- DNA Engine Dyad® and Dyad Disciple™ Peltier thermal cyclers flier (bulletin 5221)
- PTC-100® Peltier thermal cycler flier (bulletin 5223)
- Moto Alpha™ motorized heated lid flier (bulletin 5244)
- MJ Mini™ thermal cycler and MiniOpticon™ real-time PCR system brochure (bulletin 5262)

Microarray Products

- GeneGazer™ bioinformatics software flier (bulletin 5214)

Expression Proteomics

- EXQuest™ spot cutter brochure (bulletin 3194)

Electrophoresis

- Experion™ automated electrophoresis system flier (bulletin 3186)
- PowerPac™ HV high-voltage power supply brochure (bulletin 3189)
- The Experion system: Bio-Rad applies microfluidics to automate gel electrophoresis (bulletin 5285)

Chromatography

- GelTec™ process chromatography columns product information sheet (bulletin 3129)
- EasyPack™ process chromatography columns product information sheet (bulletin 3130)
- CHT™ ceramic hydroxyapatite, 40 µm — optimized packing methods in GelTec columns (bulletin 3199)

Multiplex Suspension Array Technology

- Detection of phosphorylated and total ERK and p38 MAPK by Bio-Plex™ assay, ELISA, and western blotting (bulletin 3141)
- Development of a multiplex bead-based assay for antibody screening of a nonhuman primate colony on the Bio-Plex system (bulletin 3192)

The Unmistakable Leader

Whether your research includes everyday imaging of PCR products or more demanding applications such as chemiluminescent western blots, Bio-Rad is the worldwide leader in providing quality imaging products.

Introducing the Gel Doc™ XR System

- 1.4 megapixel resolution
- Motorized lens for “hands-free” gel documentation
- Easy workflow and analysis with Quantity One® software
- FireWire interface
- PC and Mac compatible

Applications
Nucleic acid gels
1-D protein gels
Colorimetric blots
Densitometry
Colony counting

For more information, visit us on the Web at **www.bio-rad.com/products/imaging/**

FireWire and Mac are trademarks of Apple Computer, Inc.
Practice of the patented polymerase chain reaction (PCR) process requires a license.

Visit us on the Web at **discover.bio-rad.com**
Call toll free at 1-800-4BIORAD (1-800-424-6723); outside the US, contact your local sales office.

BIO-RAD

The MJ Line of Amplification Products

The perfect combination.

Bio-Rad doubles your capacity for real-time PCR.

The Chromo4™ real-time detector now offers even more flexibility. Now you can mount two Chromo4 modules on the dual-bay Dyad Disciple™ thermal cycler, doubling experimental options and output. With the Dyad Disciple base, two different protocols can be run simultaneously; you can get results sooner. Best of all, any combination of swappable Chromo4 modules and Alpha™ sample blocks can be operated in parallel, for the utmost in economy and flexibility.

- Twice the flexibility
- Twice the throughput
- 4-color multiplexing capability
- Thermal gradient feature
- Relative gene expression analysis software

For more information, visit us on the Web at **www.mjr.com**

Two Chromo4 real-time detectors on the Dyad Disciple thermal cycler.

Visit us on the Web at **discover.bio-rad.com**
Call toll free at 1-800-4BIORAD (1-800-424-6723);
outside the US, contact your local sales office.

BIO-RAD